Universidade de Aveiro Secção Autónoma das Ciências da Saúde
2014

Ana Rita Filgueiras Ferreira

Hepatitis C virus and peroxisomes: evasion from the cellular antiviral response

O vírus da Hepatite C e peroxissomas: evasão da resposta celular antiviral

Universidade de Aveiro Secção Autónoma das Ciências da Saúde
2014

Ana Rita Filgueiras Ferreira

Hepatitis C virus and peroxisomes: evasion from the cellular antiviral response

O vírus da Hepatite C e peroxissomas: evasão da resposta celular antiviral

Thesis submitted at University of Aveiro to fulfil the requirements to obtain the Master degree in Molecular Biomedicine held under the scientific guidance of Dr. Daniela Maria Oliveira Gandra Ribeiro, Principal Investigator at Organelle Dynamics in Infection and Disease group at Centre of Cell Biology, University of Aveiro.

Dissertação apresentada à Universidade de Aveiro para cumprimento dos requisitos necessários à obtenção do grau de Mestre em Biomedicina Molecular, realizada sob a orientação científica da Doutora Daniela Maria Oliveira Gandra Ribeiro, Investigadora principal do grupo "Organelle Dynamics in Infection and Disease" no Centro de Biologia Celular da Universidade de Aveiro.

Apoio financeiro da FCT (FCT; PTDC-IMI-MIC/0828/2012), Centro de Biologia Celular e Departamento de Biologia da Universidade de Aveiro.

o júri

presidente

Prof. Doutora Odete Abreu Beirão da Cruz e Silva
Professora Auxiliar com agregação da Secção Autónoma das Ciências da Saúde da Universidade de Aveiro

Doutora Daniela Oliveira Gandra Ribeiro
Investigadora principal do grupo “Organelle Dynamics in Infection and Disease” no Centro de Biologia Celular na Universidade de Aveiro

Doutora Maria João Amorim
Investigadora principal do grupo “Cell Biology of Viral Infection” no Instituto Gulbenkian para a Ciência

Acknowledgments

To (Dr.) Daniela, thank you for giving me the chance of working in your laboratory and thus, of developing this project. I am grateful for all the advices, work discussions and specially for sharing your passion and enthusiasm with me. The opportunity of working with you allowed my own professional and personal enrichment. Thank you very much for this year and a half of great things.

To Cris, for sharing your knowledge with me and for having confidence on me and on my work. Thank you for the patience and for pushing me to do better. Thank you very much for the friendship. I could not ask for better.

To Fátima, thank you for sharing your knowledge and for helping with our special cloning experiment.

To Ana, thank you for helping me with the crazy microporation experiments. Thank you also for providing a lot of sweet 'moments'.

To Marta, thank you for helping with the RT-qPCR experiments and for sharing your knowledge.

To Maria, thank you for your help with the confocal microscopy.

To Dr. Kagan, thank you for providing the cells and constructs used in this work. Thank you also for sharing your knowledge in the valuable work discussions.

To everyone in 'lab', for welcoming me and helping me to feel integrated so quickly. Thank you all for sharing the lab trips, lab dinners and a lot of good moments. Great team!

To Débora, thank you for the company during experiments and outside of "lab".

To all my friends from CBM and Molecular Biomedicine for sharing this journey with me and turning it a lot easier. A special thank you to Sandra for the company during the thesis' writing phase.

To the "special ones" (Catarina, Leonor, Inês, Vilaça and Johny), thank you for supporting me during this challenge and also for providing good moments of relaxation. I know that I am a "pain in the …".

Por fim, não posso deixar de agradecer à minha família, pelo apoio incondicional, especialmente aos meus pais porque, na verdade, sem eles eu não teria chegado onde estou agora.

I also have to thank to Daniela and Dr. Friedeman for allowing me to spend some months in Germany as an ERASMUS student. With this opportunity I had the chance to test myself in a new experience. Thanks to all the colleagues and friends that I had the opportunity to meet during these 3 months.

keywords

Peroxisomes, Hepatitis C , viral infection, cellular antiviral response, MAVS, NS3/4A

abstract

Hepatitis C virus (HCV) causes the most prevalent viral infection worldwide. Upon infection, the HCV genome is detected by the RIG-I-MAVS signalling pathway leading to the production of direct antiviral effectors. NS3/4A protease is the main inhibitor of innate immunity against HCV and it was found to inhibit the mitochondrial signalling protein (MAVS).

MAVS was recently found to localize at peroxisomes coordinating with mitochondria the activation of effective antiviral response. Peroxisomal MAVS is responsible for inducing a rapid but short termed antiviral response that is IFN-independent, contrary to mitochondrial MAVS which is associated with the activation of an IFN-dependent antiviral response with delayed kinetics.

With this work we aimed at evaluating the effect of NS3/4A over the peroxisomal–MAVS pathway. Our results showed that the MAVS localizing exclusively at peroxisomes is targeted by the HCV NS3/4A protease. We also show that the MAVS cleavage by NS3/4A impaired the antiviral response mediated by peroxisomal-MAVS.

These results reaffirm the importance of peroxisomes for viral-host interaction and in antiviral defences. Further studies are proposed in order to better understand the role of this organelle in innate immunity. These may lead to the improvement of therapy against HCV infection.

palavras-chave

Peroxissomas, Virus da Hepatite C, infeção viral, resposta antiviral celular, MAVS, NS3/4A

resumo

O vírus da hepatite C (VHC) provoca a infeção viral mais prevalente em todo o mundo. Após infeção, o genoma do VHC é detetado pela via de sinalização RIG-I-MAVS levando à produção de efetores diretos da resposta antiviral. A protease NS3/4A é o principal inibidor da resposta imune produzido pelo VHC e foi descrito como inibidor da proteína MAVS.

A proteína MAVS foi recentemente localizada nos peroxissomas que, juntamente com a mitocôndria, coordenam a resposta antiviral. A MAVS peroxisomal é responsável pela indução de uma resposta antiviral rápida mas de curta duração que é independente de interferões, mas pelo contrário, a MAVS mitocondrial está associada a uma ativação da resposta antiviral que é dependente de interferões mas que se caracteriza por uma cinética retardada.

O nosso objetivo com este trabalho consistiu em avaliar o efeito da NS3/4A na via de sinalização coordenada pelos peroxissomas. Os nossos resultados mostram que a MAVS localizada nos peroxissomas é alvo da protease NS3/4A do VHC. Também mostramos que a clivagem da proteína MAVS pela NS3/4A inibe a resposta antiviral mediada pela MAVS peroxissomal.

Estes resultados reafirmam a importância dos peroxissomas na interação vírus-hospedeiro e na defesa antiviral. Futuros estudos são aconselhados para que se compreenda a função dos peroxissomas na imunidade inata. Estes podem levar a uma melhoria na terapia da infeção pelo VHC.

List of abbreviations

aa	amino acids
acetyl-CoA	acetyl coenzyme A
AP-1	activator protein 1
ATP	adenosine-5'-triphosphate
CARD	caspase activation and recruitment domain
CARDIF	card adaptor inducing IFN-β
CLDN1	claudin-1
Cys	Cysteine
DAAs	directing acting antiviral agents
DC-SIGN	dendritic cell-specific intercellular adhesion molecule-3-grabbing non-integrin
DLP1	dynamin-like protein 1
DNA	deoxyribonucleic acid
ds	double-stranded
ER	endoplasmic reticulum
ESCRTs	endosomal sorting complex required for transport
Fis1	mitochondrial fission 1 protein
GAGs	glycosaminoglycans
H_2O_2	hydrogen peroxide
HCV	Hepatitis C virus
IFNs	Interferons
IKK	inhibitor of κB kinase
IPS-1	IFN-β promoter stimulator 1
IRES	internal ribosomal entry site
IRF	interferon regulator factor
ISGs	interferon-stimulated gene
KO	knock-out
LD	lipid droplet
LDLR	low-density lipoprotein receptor
LGP2	laboratory of genetics and physiology 2
L-SIGN	liver/lymph node-specific intercellular adhesion molecule-3-grabbing integrin
LVPs	lipoviral-particles

MAM	mitochondria-associated membranes
MAVS	mitochondrial antiviral signalling
MDA5	melanoma differentiation-associated gene-5
MEF	mouse embryonic fibroblast
Mff	mitochondrial-anchored protein ligase
MTP	microsomal transfer protein
NF-κB	nuclear factor kappa-light-chain-enhancer of activated B cell
nt	nucleotides
PAMP	pathogen-associated molecular pattern
peg-IFN-α	pegylated interferon α
Pex	Peroxin
PMP	peroxisomal membrane protein
PPREs	peroxisome proliferator response elements
PRR	pattern recognition receptor
PPR	peroxisome proliferator activated receptor
PTS	C-terminal peroxisomal targeting signal
RdRp	RNA-dependent RNA polymerase
RIG-I	retinoic acid-inducible gene I
RLR	RIG-I like receptors
RNA	ribonucleic acid
RNS	reactive nitrogen species
ROS	reactive oxygen species
RXRs	retinoid X receptors
SR-BI	scavenger receptor class B type I
ss	single-stranded
SVR	sustained virological response
TBK1	TANK-binding kinase 1
TRAF	tumor necrosis factor (TNF) receptor-associated factor
UTR's	untranslated regions
VISA	virus-induced signalling adaptor
VLCFAs	very long chain fatty acids
VLDL	very-low-density-lipoproteins

Index

List of tables

List of figures

I. Introduction

I. Introduction

1.1 Hepatitis C Virus

1.1.1 Epidemiology and Classification

Hepatitis C virus (HCV) was discovered in 1989 as a cause of non-A and non-B post-transfection hepatitis (1). Nowadays it is one of the most prevalent infections worldwide and, according to the World Health Organization, 130 to 170 million people are currently chronically infected and 3 to 4 million people are newly infected each year (2). The acute infection is normally asymptomatic and 85% develop chronic infection. Chronic infection induces chronic hepatitis, liver fibrosis and cirrhosis which may evolve later to hepatocellular carcinoma (3).

HCV has been classified as part of the *Hepacivirus* genus from the *Flaviviridae* family. HCV is subdivided in 6 genotypes that differ according to geographic distribution, specific symptoms and treatment response. Each genotype can be further divided in subtypes (e.g. 1a, 1b, 2a) (4). The current treatment is based on a combined therapy of pegylated interferon α (Peg-IFN-α) and ribarin. Peg-IFN-α induces a cellular antiviral state while ribarin acts in a synergistically manner throw different mechanisms (e.g. modulation of interferon-stimulated gene (ISGs) expression or error catastrophe induction by mutagen incorporation) (5). For unknown reasons this therapy is less effective in infections caused by genotype 1 (sustained virological response[1] less than 42%-52%) compared with genotype 4, 5 or 6 (SVR 65%-85%) and genotype 2 or 3 (SVR 76%-80%) (6). Recently, direct acting antiviral agents (DAAs), such as NS3 protease and RNA polymerase inhibitors, were developed and when one of these is combined with the standard therapy, the SVR increases to 70% (7). This triple combination is only allowed in genotype 1 infected patients (8). However, patients can develop resistance due to numerous variants (quasi-species) that are produced during HCV replication because of the high replication rate and low fidelity of HCV RNA-dependent RNA polymerase (6). Until now no vaccine is available due to the high genetic variability of this virus (9).

[1] Sustained Virological Response (SVR) corresponds to an undetectable viral load six months after termination of treatment.

1.1.2. Genome

HCV is characterized as a hepatotropic enveloped positive single-stranded RNA virus. It has a 9.6 kb genome composed by an open reading frame, that encodes a polyprotein of 3000 amino acids (aa), flanked by 5' and 3' untranslated regions (UTR's) at both ends that are highly structured structures essential for replication and translation. The 5' UTR with 341 nucleotides (nt) allows the cap-independent translation of viral RNA since it contains an internal ribosomal entry site (IRES) that is capable of binding to the 40S ribosomal subunit leading to the formation of a stable pre-initiation complex (10). The 3' UTR length can vary between 200-235 nt and its function is crucial for RNA replication (11).

1.1.3. Structure and life cycle

HCV studies are difficult to perform due to its viral low titters and poor stability (12). Nonetheless, in the last few years several techniques have emerged which allow the study of HCV infectivity. The first studies about HCV were possible due the development of functional cDNA clones that allowed the first molecular characterization (13). Meanwhile, HCV replication systems that used drug-selectable 'subgenomic replicons' were established and permitted study of the intracellular steps of HCV replication without producing infectious particles (14,15). Recently, reverse-genetics cell culture systems for HCV have been developed which allow the production of infectious virions in cell culture (designated HCVcc particles) (14). Through the association of these techniques with electron microscopy studies, advances in morphological studies of HCV particles were possible.

HCV particles are different from other members of the *Flaviviridae* (16). HCV presents a highly heterogeneous structure with a proximal size ranging between 40 to 100 nm in diameter (≈50 nm in other members), a spherical morphology that differs from the *Flaviviridae* icosahedrical symmetry (12,17) as well as a low density oscillating between 1.06 g/mL to 1.25 g/mL (18). However, these characteristics are also variable between virus particles generated in cell culture or isolated from infected patients (19).

HCV primarily infects hepatocytes cells of humans and chimpanzees having, however, the capacity to spread through B cells, dendritic cells and other cells already reported (20). For entry, several potential host proteins were already proposed including the receptors human tetraspanin CD81, scavenger receptor class B type I (SR-BI), claudin-1 (CLDN1), mannose binding lectins DC-SIGN (dendritic cell-specific intercellular adhesion molecule-3-grabbing non-integrin) and L-SIGN (liver/lymph node-specific intercellular adhesion molecule-3-grabbing integrin), and the binding

factors glycosaminoglycans (GAGS) and low-density lipoprotein receptor (LDLR) (21). Despite all the molecules described above being important and necessary for HCV entry, none of them alone is sufficient (22).

The more recent model of HCV entry into hepatocytes explains that HCV particles bind to GAGs and LDLR until the SRB1 recognizes the HCV E2 proteins and the virion-associated lipoproteins. The recognition exposes CD81 binding sites to HCV E2 inducing the formation of a CD81-CLDN1 complex that has the capacity to activate the clathrin-mediated endocytosis. However, the mechanism of endocytosis induction has to be further investigated (23).

Following internalization, HCV induces a low pH environment inside the endosome which triggers the fusion process through the rearrangement of HCV glycoproteins. The mechanisms behind the HCV low pH –induced fusion still have to be elucidated, although it is believed that it is associated to the endosome lipid composition (20,23). Consequently, these processes lead to viral RNA release to the cytosol where it will be translated and replicated.

HCV translation initiates after the release of genomic RNA into the cell cytoplasm where viral positive-strand HCV RNA will serve as template for HCV polyprotein synthesis in the rough ER (Figure 2). IRES, present in the 5' UTR, is the key in this process inducing the formation of a stable pre-initiation complex by binding to the 40S ribosomal subunit. Subsequent recruitment of the eukaryotic initiation factor (eIF) 3 and the ternary complex eIF2-GTP-Met-tRNAi results in the formation of the 48S like complex. After hydrolysis and release of eIF2-GDP and eIF3, 60S ribosomal subunit binds to form the 80S complex (24,25). This complex has the capacity to continue with elongation and termination leading to viral protein translation. Translation seems to be influenced by viral proteins such as core protein, NS4A and NS5B (10,20) as well as by the 3'-UTR and cellular factors (24).

HCV RNA translation leads to the production of a large polyprotein precursor, which is processed co- and post-translationally into 10 viral proteins (Figure 1). The polyprotein can be separated in two regions the N-terminal that encodes the virion structural proteins, the highly basic core (C) protein and envelop glycoproteins E1 and E2, which are followed by the small integral membrane protein p7 that is not a component of virion structure (detailed functions on Table 1). The C-terminal encodes the non-structural (NS) proteins NS2, NS3, NS4A NS4B, NS5A and the NS5B, each are responsible for the intracellular processes of the virus life cycle (detailed functions on Table 1). The maturation of the structural proteins is possible through host signal peptidases cleavage but within the NS region the cleavage is processed by two viral enzymes, the NS2

autoprotease and the NS3/4A serine protease (26). HCV translation also produces another protein by ribosomal frame shift within the core gene, named F (frame shift) or ARFP (alternative reading frame protein) (26).

Table 1 | Function of Hepatitis C Virus (HCV) proteins and virus cycle significance (27,28)

HCV protein	*Function*	*Virus cycle significance*
E1	Envelop Fusion domain	Entry
E2	Envelop Receptor Binding Fusion domain	Entry
Cores	Nucleoprotein RNA binding Immune modulation Autophagy	Assembly of the viral nucleocapsid
p7	Calcium ion Channel (viroporin)	Viral assembly Release
NS2	NS2/3 autoprotease	Viral assembly
NS3	Component of NS2/3 and NS3/4A NTPase/helicase Serine protease RNA helicase	HCV processing Immune modulation Replicase complex
NS4A	NS3/4A proteinase cofactor	NS3 targeting to the ER membrane
NS4B	Remodeling od host-cell membranes	Membranous web induction
NS5A	RNA replication by complexes formation	
NS5B	RNA-dependent RNA polymerase	Replicase complex

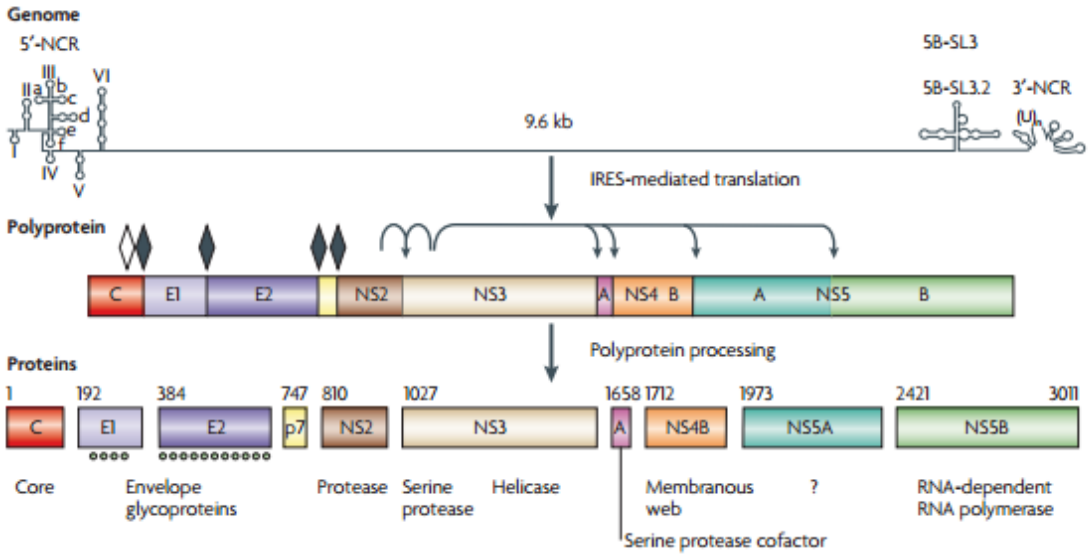

Figure 1 | Hepatitis C virus (HCV) genome organization and polyprotein processing (20). HCV RNA genome is represented at the top. Genome translation into a polyprotein precursor is mediated by the internal ribosome entry site (IRES).HCV polyprotein contains all the non-structural and structural proteins of HCV that has to be cleaved to release mature proteins. The diamonds indicate the cleavage sites for host signal peptidases. Arrows indicate cleavage sites for NS2 and NS3/4A proteases. Dots indicate glycosylation of envelope proteins.

Replication Complex

NS4B expression induces alterations in cell membranes leading to the formation of 'sponge-like inclusions' closely associated to rER and designated as membranous web (Figure 2) (29,30). These type of structures are induced by all positive-strand RNA viruses, including HCV, and they are composed by structural and non-structural proteins, replicating RNA, and altered host-cell membranes (30). This strategy seems to offer several advantages to viruses (30,31) such as (i) compartmentalization and concentration of viral products in one place, (ii) replication complex organization as well as physical support, (iii) tethering of viral RNA during unwinding, (iv) supply of lipid constituents important for replication, and (v) protection of viral RNA from host defences. During HCV replication, NS5B is the main character being the RNA-dependent RNA polymerase (RdRp) necessary for the synthesis of a complementary negative-strand RNA intermediate, that will serve as a template to create several copies of the genomic positive-strand RNA. For acting as RdRp, NS5B is dependent of its transmembranar domain (32). It was found that the NS3 protein may also be important for RNA replication by complementing the action of NS4B in inducing the membranous web, as well as through binding to RNA. NS3/4A has a DExH/D-box helicase domain that allows the binding to nucleic acids after ATP hydrolysis. This function could be important for separation or unwinding of local RNA or dislocation of RNA-binding proteins (8). It seems that NS5A phosphorylated state can regulate the RNA replication directly or indirectly through the binding to host proteins that are implicated in replication (33). Several host factors have been proposed as regulators of HCV RNA replication, including the availability of fatty acids (25,26,34).

Regarding to NS5B's activity as RdRp, it is important to refer that viral RNA RdRp do not have proofreading activity leading to a high frequency of nucleotide substitutions during replications (32). This means a high error or mutation rate and the consequence is the rapid generation of viral variants. Thus, infected individuals present heterogeneous viral microvariants of a predominant master sequence, referred as quasispecies (32,35). The existence of such a heterogeneous variants or quasispecies is associated with different biological properties and phenotype in the host, such as carcinogenicity or tissue tropism. Additionally, it seems to be correlated with resistance to IFN therapy whereas some quasispecies are more resistant to therapy than others (35).

Replication and translation relationship

HCV positive-strand RNA virus possesses the regulator elements for both replication and translation. Both 5' and 3' UTR elements induce and regulate replication and translation processes

in the same RNA molecule. For replication, the positive-strand RNA has to be converted in a complementary negative-strand RNA and this processes goes from 3' to 5'. However, translation occurs in the same genome positive strand RNA in the opposite direction, from 5' to 3' (25). Thus, HCV replication and translation have to be closely regulated.

In other positive-strand RNA viruses it was found that one of the processes was preferred comparing with the other. In the case of poliovirus, it has been reported that transcription was dependent on the translation activity whereas the translation of Sindbis virus or vesicular stomatitis virus has been reported to be transcriptionally dependent (25). In HCV, it was found that RNA translation was dependent on active RNA synthesis. In one study, the inhibition of RNA synthesis decreased the HCV viral protein synthesis before a significant decrease in the amount of RNA had occur (36). Several proteins have been identified as possible regulators of the balance of these two processes, such as viral and host proteins (e.g. core protein or PKR, respectably) (25).

Assembly and release

Several theories about HCV assembly exist but all of them stress the interplay between the assembly process and the lipid metabolism (19). After post-translation modifications, the core protein is transported to LDs and induce its relocation in cells, changing its general distribution in the cytosol to a close nuclear subcellular location. Like this, LDs become closer to ER and to an ER-like membranous web where replication occurs (37). Although it is unknown how the interaction occurs, it is recognized that NS5A associated to RNA becomes close enough to allow the oligomerization between core protein and HCV genome (38). This interaction allows nucleocapsid formation (39).

Nucleocapsids have to be encapsulated and acquire viral glycoproteins at the surface to become infectious viral particles. The mechanism through which it occurs is not yet established. The current models for envelopment suggest that nucleocapsids are incorporated in ER lumen where they obtain their lipid envelope by incorporation into the very-low-density-lipoproteins (VLDL) pathway (19). VLDL, as well LDL (low-density lipoproteins), are the major transporters and are produced and released by hepatocytes into the blood. Their architecture is similar to LDs: they are composed by a core full of triglycerides and cholesterol esters which is surrounded by a layer of apolipoproteins and phospholipids (40). During circulation in the blood stream they are converted into LDL due to exchange of lipids with tissues (41). In hepatocytes, they form in the ER lumen through a multistep process. Initially, apoB suffers lipidification during its transport by microsomal transfer protein (MTP) inside the ER lumen, forming the VLDL precursor (pre-VLDL). Further

lipidification of the pre-VLDL occurs within the secretory pathway forming VLDL particles, although the mechanisms behind it are yet to be clarified. It was hence proposed that HCV nucleocapsids somehow interact with VLDL incorporating the same proteins, apoB, apoE and MTP. This is corroborated with the findings that circulating HCV virions are associated with apoB and apoE and others constituents of VLDLs, this particles are termed LVPs (lipoviral-particles) (42).

Glycoproteins E1 and E2, after translation form a non-covalent heterodimer which are retained in the ER lumen until HCV assembly (41). Hence, some models suggest that they are incorporated while the nucleocapsid envelopment occurs inside ER lumen. Some studies showed that their incorporation may be apoB- and apoE- dependent (19,41,43). Throughout the secretory pathway they suffer maturation and form large covalent complexes in the HCV virions surface, essential for HCV entry (39).

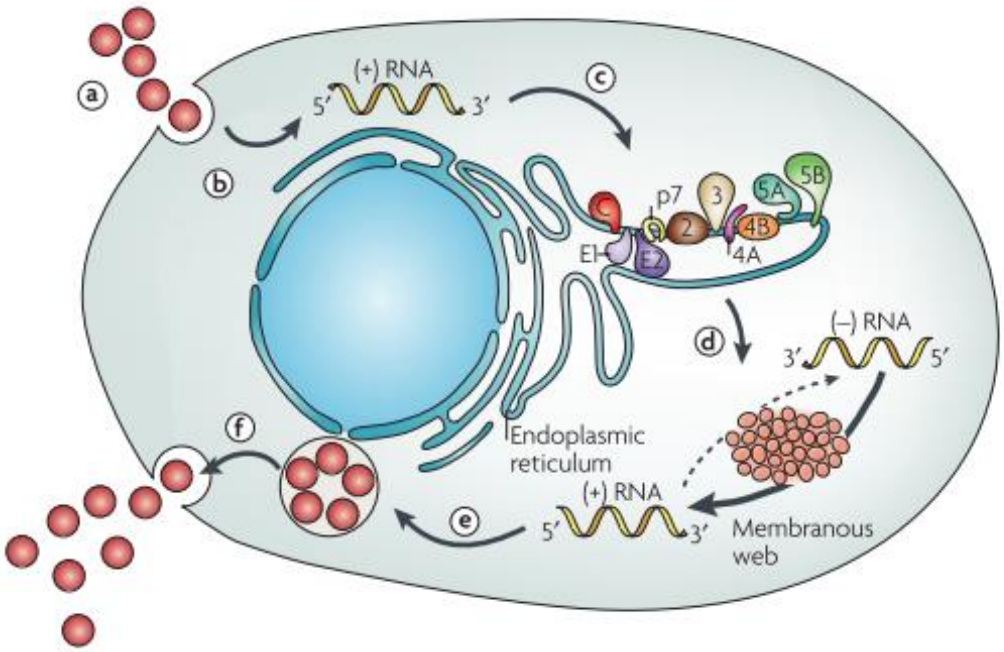

Figure 2 | Hepatitis C virus life Cycle (20). After HCV entry into the cell (a) and uncoating (b), the HCV genome is release into the cytoplasm. Translation is mediated by IRES (c) and polyprotein processing as well as RNA replication occurs (d). Packing and assembly (e) is followed by virion maturation and release (f). It is important to refer that translation, replication and membranous web formations are represented as separated steps only for simplicity. These are tightly correlated processes that may occur in parallel.

HCV virion budding occurs through the endosome secretory pathway that is regulated by ESCRTs (endosomal sorting complex required for transport) (41,43). The ESCRT pathway is responsible for the budding and fission of membranous compartments that curve away from the cytosol by incorporating target proteins into a multivesicular body for degradation. It is used by many enveloped viruses to bud into extracellular compartments. Through this pathway HCV release

does not require cell lysis and takes advantage of host cell excretory pathway to get out of the cell.

1.1.5. HCV NS3/4A protease

NS3/4A protein is a non-covalent heterodimer complex formed by two HCV proteins, NS3 serine protease and NS4A cofactor (44). In the N-terminal NS3 contains a serine protease and a NTPase/RNA helicase in the C-terminal (45). For NS3 activation and optimal function, NS4A protein binding is essential as it alters NS3 conformation stabilizing the catalytic centre. Several studies demonstrated that any substitutions in NS4A sequence lead to a decrease in NS3 activity (44). NS4A also has the function of tethering the holoenzyme complex to intercellular membranes (46). Hence, NS3 protein confers the catalytic function and NS4A consists in the activation subunit of this complex.

NS3/4A is essential for HCV life cycle not only in HCV replication but also for its persistence and pathogenesis. During HCV polyprotein processing, this complex is responsible for the proteolytic cleavage of four junctions of HCV polyprotein precursor leading to the maturation HCV non-structural proteins (NS3-4A self-cleavage, NS4A-NS4B, NS4B-NS5A, NS5A-NS5B) (Figure 1) (47). As indicated in the previous sections, NS3/4A also intervene in HCV genome replication as well as in viral assembly processes.

NS3/4A complex is also essential for HCV evasion to host cellular defences (44). Several studies have shown that NS3/4A blocked TLR3 and RIG-I pathways impairing the induction of IFN-antiviral response at the cellular level (for further details read the next section) (46,48). Moreover it was found that NS3/4A also inhibits the systemic innate immunity through the cleavage of the complement system component 4, mainly produced by hepatocytes (49,50).

1.2. Innate Immune Response

The innate immune system expresses different pattern recognition receptors (PRRs) that recognize essential compounds of the pathogen's structure, named pathogen-associated molecular patterns (PAMPs) (51). PRRs can be associated to cell membranes (membrane-bond PRR), intracellular compartments (cytosolic PRR), secreted into the blood stream or into tissue fluids (secreted PRR and phagocytic PRR) (50,52). These receptors have as main functions the

opsonisation of pathogens, activation of complement and coagulation cascades, phagocytosis, activation of proinflammatory signalling pathways and induction of apoptosis (52).

1.2.1. Cellular Antiviral Defence

Viruses are highly infectious microorganisms completely dependent on the host cell machinery. Viruses exploit and reprogram the host metabolism to replicate, which can lead to the host's death. However, throughout evolution, viruses and host co-existence always has been dependent of each other's survival, resulting in a gain of strategies to antagonize each other and promote their own survival (53).

Viral infection induces a set of intracellular responses that results in the production of antiviral molecules that compose the first line of immune defence. The host response to infection aims to abort viral replication and inhibit virions production, constricting infection to other cells (52). Intracellular PRRs recognize viral PAMPs that mainly consist of viral nucleic acids, such as 5' triphosphate terminal RNA and the presence of DNA in cytoplasm, with specific signatures, allowing the differentiation between non-self and host nucleic acids (52,54). This recognition is possible due to a variety of receptors, such as the endosomal Toll-like receptors (55,56), cytosolic DNA sensors and the cytosolic RIG-I-like family (RLRs) (57).

Toll-like receptors were first discovered in drosophila embryos and their important role in immune defence against bacterial and fungal infections was establish in adult fly's (58). Mammalian homologs were identified later, existing 10 TLRs in humans and 13 TLRs in mice. These TLRs differ in ligand specificity, expression pattern and target genes – TLR1, TLR2, TLR4, TLR5, and TLR6 are present in plasma membrane and the TLR3, TLR7, TLR8, TLR9 are present at endosomal membrane. In viral infection, additionally to viral nucleic acids recognition by endosomal TLR - TLR3 recognize dsRNA, TLR7 and TLR 8 ssRNA and TLR9 recognizes CpG DNA - the TLR2 and TLR4 present at the plasma membrane can also recognize viral proteins from the viral external structure (54,58). TLR activation by PAMPs culminates in the activation of transcription factors through the activation of a variety of adaptor molecules, which differ according to the specific TLR that induces the cascade. These transcription factors regulate the expression of interferon, cytokines and chemokines and also seem to influence cellular maturation and survival (54).

In eukaryotic cells, DNA is confined within the nucleus and mitochondria, thus the presence of DNA in cytoplasm is an aberrant situation. There is a variety of cytosolic DNA sensors that

recognize non-self B-form dsDNA that is common to viruses, bacteria and apoptotic cells. This recognition induces a robust immune response, including inflammasome activation and type-I IFN expression (59). Some of these receptors were identified: DAI and STING, that stimulate the TBK1-IRF3 axis after recognition of dsDNA; RNA polymerase III (Pol III), which uses AT-rich and herpesvirus dsDNA as a template for 5' triphosphate RNAs production; PYHIN family, a group of proteins that possess a domain capable of DNA binding and a domain that allows protein-protein interactions, including AIM2 and IFI16 proteins. Concerning viral recognition by cytosolic DNA sensors, the specific sensor that mediates recognition is dependent of the expression pattern of these in each cell type (60).

RIG-I-like family

RIG-I-like receptors (RLR) family consists in three molecules termed retinoic acid-inducible gene (RIG-I), melanoma differentiation-associated gene-5 (MDA5) and laboratory of genetics and physiology 2 (LGP2) (57). They are characterized by a DExD/H-box helicase domain. RIG-I and MDA5 also contain an N-terminal tandem caspase activation and recruitment domain (CARD). RIG-I, MDA5 and LGP2 have a C-terminal domain (CTD, known also as RD=repressor domain).

During viral infection, RIG-I and MDA5 can recognize viral RNA released into the cytosol. This recognition is mediated by the DExD/H-helicase box domain and triggers the production of type-I IFN (61). The RD of RIG-I inhibits the activation of the downstream signalling being necessary the activating ligand in order to induce a conformational alteration to expose the RIG-I CARD domains (54,62). Opposing to RIG-I, MDA5 does not undergo a conformational alteration, being the CARD domains permanently exposed. LGP2 function in immune response is not well understood. The lack of CARDs and the presence of helicase and CTD suggests a possible regulatory function. Some studies indicate that LGP2 can either enhance or inhibit the function of RIG-I and MDA5 (8).

RIG-I and MDA5 have specific ligands that allow specific viral recognition (Figure 3). RIG-I recognizes viral genome that contains 5'-triphosphate ssRNA, base pairing at the 5'-end due to secondary dsRNA structures or short RNA sequences while MDA5 recognizes long or with high molecular weight dsRNA sequences.

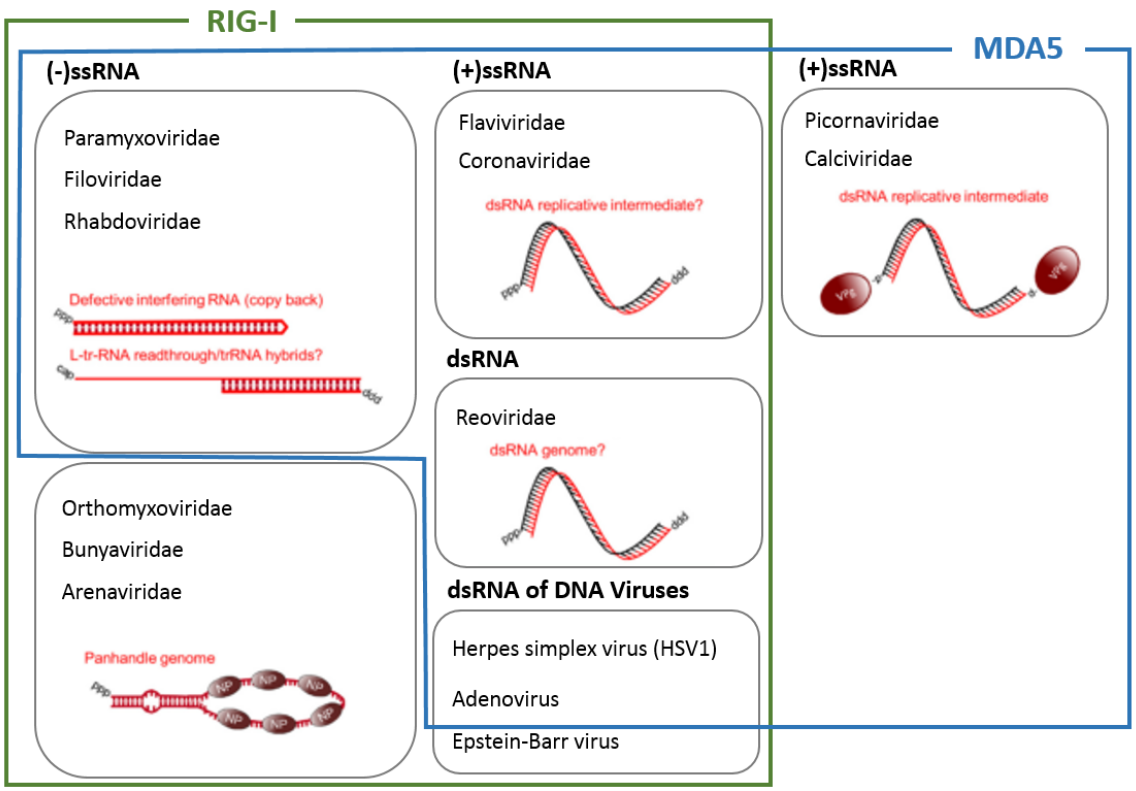

Figure 3 | Viruses recognized by RIG-I and MDA5 and evasion to RLR recognition (Adapted from Schlee M. 2013) (8). ss: single stranded, ds: souble stranded, (+): positive strand genome, (−): negative strand genome

MAVS Signalling

Mitochondrial antiviral signalling (MAVS (63), also known as card adaptor inducing IFN-β=CARDIF (64), IFN-β promoter stimulator 1=IPS-1 (65) or virus-induced signalling adaptor=VISA (66)) was described as an adaptor protein with 540 aa in the RLR antiviral pathway. MAVS N-terminal contains a CARD-like domain and a proline-rich region, whereas the C-terminal consists in a hydrophobic transmembrane domain that targets the protein to the respective intracellular membranes (mitochondria (63), peroxisomes (67), and mitochondria-associated membranes (MAM) (68)). Deletion studies revealed that both N-terminal CARD domain and C-terminal are essential for MAVS function (63). Upon RIG-I activation by viral RNA recognition, MAVS is activated by receiving the RIG-I stimulus through the CARD domain. MAVS activation induces the formation of a detergent-resistant oligomers that may involve the CARD domains of several MAVS (63,69,70).

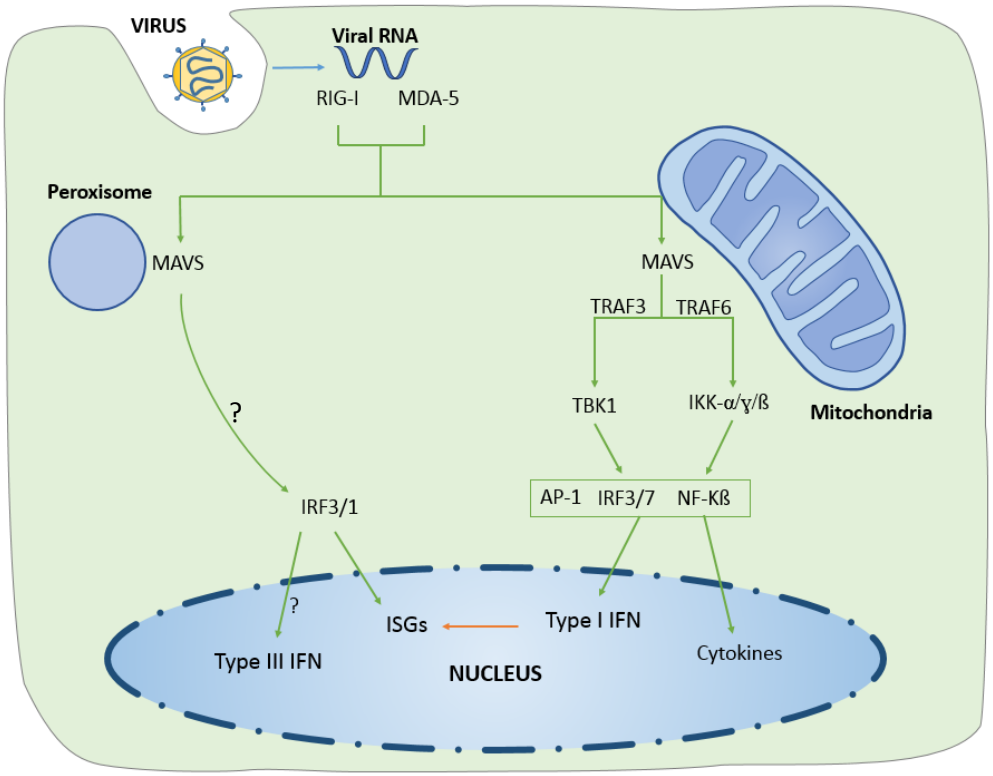

Figure 4 | Schematic representation of MAVS pathway (67,71,72). RIG-I and/or MDA5 recognize viral RNA which leads to MAVS activation through CARD domains interaction. Mitochondrial-MAVS pathway triggers the expression of type I IFNs through the formation of an enhanceosome composed by the transcription factors AP-1, IRF3, IRF7 and NF-κB. These transcription factors are activated by the kinases TBK1 and IKK. Peroxisomal-MAVS pathway induces the dimerization of IRF3 with IRF1 that are essential for direct and IFN-independent ISGs expression. Peroxisomal MAVS may have a role in type III IFN expression.

MAVS is present in the outer membrane of mitochondria (63), peroxisomes (67), and mitochondria-associated membranes (MAMs), which interconnects mitochondria and peroxisomes (68). The signalling pathway downstream of MAVS remains to be fully understood, being the mitochondrial-MAVS pathways better described. However, it has already been identified that both peroxisomal and mitochondrial MAVS have specific signalling pathways which result in a different but complementary response (67). Peroxisomal MAVS is associated to a rapid but short-termed induction of interferon stimulated genes (ISGs) that it is IFN-independent while mitochondrial MAVS is responsible for the production of ISGs in a IFN-dependent manner with delayed kinetics (67). In the mitochondrial MAVS pathway some downstream molecules were already identified (Figure 4). MAVS oligomerization induces via TRAF6 and/or TRAF3, the activation of TBK1 and IKK kinases. These kinases are responsible for regulating the transcription factors that form the enhanceosome (NF-κB, interferon regulatory factor (IRF) 3 and 7, and AP-1)

that activates type I IFNs expression (73). Regarding the peroxisomal MAVS a lot is still to be investigated but a new study shed some light over the downstream effectors of peroxisomal-MAVS pathway (Figure 4) (71). When MAVS was discovered at peroxisomes it was also revealed that IRF1 may take a role in the direct and IFN-independent induction of ISGs, through dimerization with IRF3 (67). Later it was also demonstrated that RLR could drive type III IFN expression through peroxisomal-MAVS pathway and IRF1 could be the regulator of this response (71). It was accepted that peroxisomal MAVS could drive the activation of NF-κB and IRF3 that in coordination with other pathways can promote the formation of the enhanceosome and prelude in type I IFNs expression. However, is still unknown how these different responses are coordinated and how they induce different cellular responses in the fight against viruses (71).

1.2.2. Cellular antiviral response to HCV and viral evasion

HCV infection is mainly sensed by RLR family and TLR3.These PRRs sense dsRNA that accumulates in cytoplasm during infection or that is present inside the endosome by uptake of dying cells. This recognition activates specific signalling cascades that culminate with IFN-β and proinflamatory cytokine production through the induction of antiviral and immunomodulatory genes. Type III interferons are also activated, however the activation mechanism is not well understood. It was already described that this immune response to HCV infection is set rapidly, even before extensive viral synthesis (74). IFNs production induces the production of ISGs and several of these were already associated to the suppression of HCV replication. This suppression is possible due to the action of multiple ISGs that target different steps of HCV life cycle (e.g. IRF1 acts in HCV translation and RNA replication but viperin only acts against RNA replication) (75).

During acute HCV infection and in cases of high initial viremia, HCV can be cleared spontaneously, suggesting that a rapid response of PRRs and innate immune induction can control acute HCV infection. However, 80% of HCV infected patients do not effectively control the virus and develop chronic infection (76). This evolution is associated with the evolutionary adaptation of HCV which developed innate immune evasion mechanisms. HCV NS3/4A protease, as already described (section 1.1.5), efficiently cleaves two important antiviral signalling molecules after HCV PAMPs recognition by host PRRs: MAVS protein of RLR pathway and TRIF, a TLR adaptor protein (77). This complex disables two important antiviral signalling pathways, inhibiting IFNs production. HCV also targets PKR, another PRR that is also activated during infection. PKR acts by suppressing host-mRNA translation and consequently viral translation is also impaired. However, HCV regulation of PKR activity is complex and it has to be further investigated (76).

Nevertheless, the innate immune system is capable of reacting to infection leading to the production of hundreds of type I and/or type III induced ISGs. This response controls the infection to some extent but it is not sufficient to eliminate HCV. Additionally, patients with high levels of ISGs do not respond to treatments with the common antivirals (78).

1.3. Peroxisomes

Peroxisomes are highly dynamic, multifunctional and ubiquitous organelles present in eukaryotic cells and play diverse metabolic roles depending on the cells type. Independent of the cell origin, all peroxisomes share the two main biochemical functions: hydrogen peroxide (H_2O_2) metabolism and fatty acid oxidation (79). Peroxisomes interact functionally and morphologically with other organelles such as ER, mitochondria and lipid droplets (80).

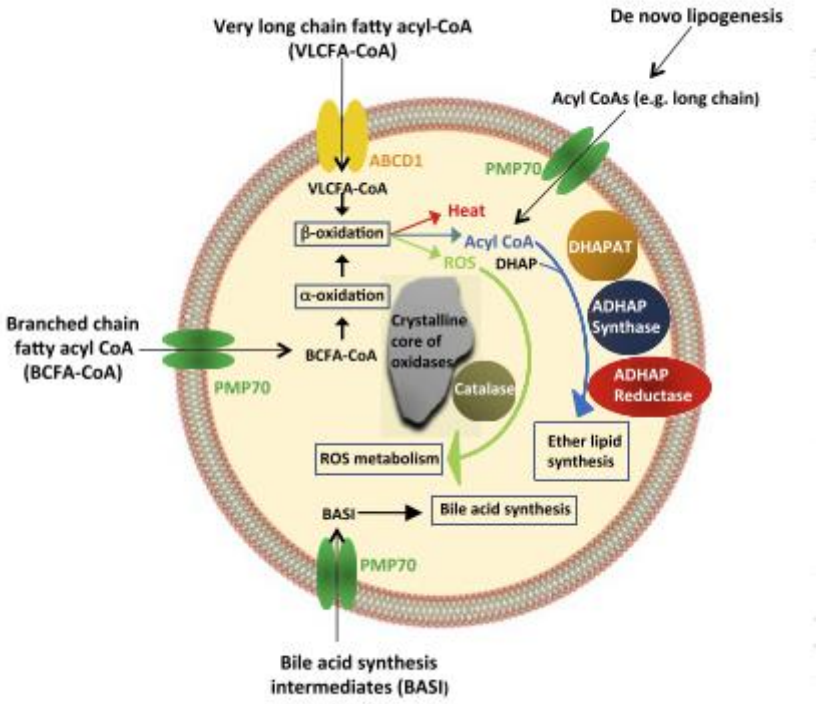

Figure 5 | Schematic view of peroxisomes structure and functions (81).

Peroxisomes' shape and size vary greatly in different tissues, ranging from a spherical to rod-like form and from 0.1 to 0.5 μm in diameter, but they can also appear as elongated tubular organelles (up to 5 μm) (81). Their structure consists in a single lipid membrane that surrounds a

granular matrix, devoid of DNA or protein synthesis machinery (Figure 5). Peroxisomes proteins are encoded by nuclear genes and synthesized in cell cytoplasm by polyribosomes (79).

Since their discovery in the 1965 a lot was learned about peroxisomes and it is now known that they are essential for human health and development (82). A group of inherited peroxisomal disorders in humans was discover and they are characterized by severe metabolic dysfunctions and neurological and developmental defects (83–85).

1.3.1. Structure

Biogenesis

Peroxisomes can arise from *de novo* formation or by growth and division from pre-existing organelles (Figure 6) (83).

The *de novo* formation of peroxisomes from ER was found after the reintroduction of deficient genes (encoding the membrane biogenesis/import factors Pex19, Pex3 or Pex16) in mutant cells lacking peroxisomes or in yeast mutants lacking peroxisomes due to a defect in segregation/inheritance (86). It was also reported that artificial targeting of Pex3 to mitochondria also induced the *de novo* synthesis of peroxisomes from mitochondria membrane, suggesting that natural or artificial targeting of Pex3 to any endomembrane may initiate peroxisome biosynthesis (87).

In mammalian cells, as well as in plants and fungi cells, peroxisomes normally multiply from growth and division where a sequence of morphological alterations occur, including elongation, membrane constriction and final fission (88). Peroxisome membrane elongation requires Pex11, a peroxisomal membrane protein (PMP). The following final fission process depends on the dynamin-related-protein GTPase DLP/DRP1 and its membrane adaptors Fis1 and MFF in mammals. This machinery is shared with mitochondria, a common feature in mammals, fungi and plants (88).

Both peroxisomal formation processes, either from ER or by growth and division, follow the same maturation process in order to convert peroxisomes in a mature and metabolic active organelle. The maturation process is achieved through the selective and stepwise import of certain PMPs, membrane lipids and matrix proteins (89).

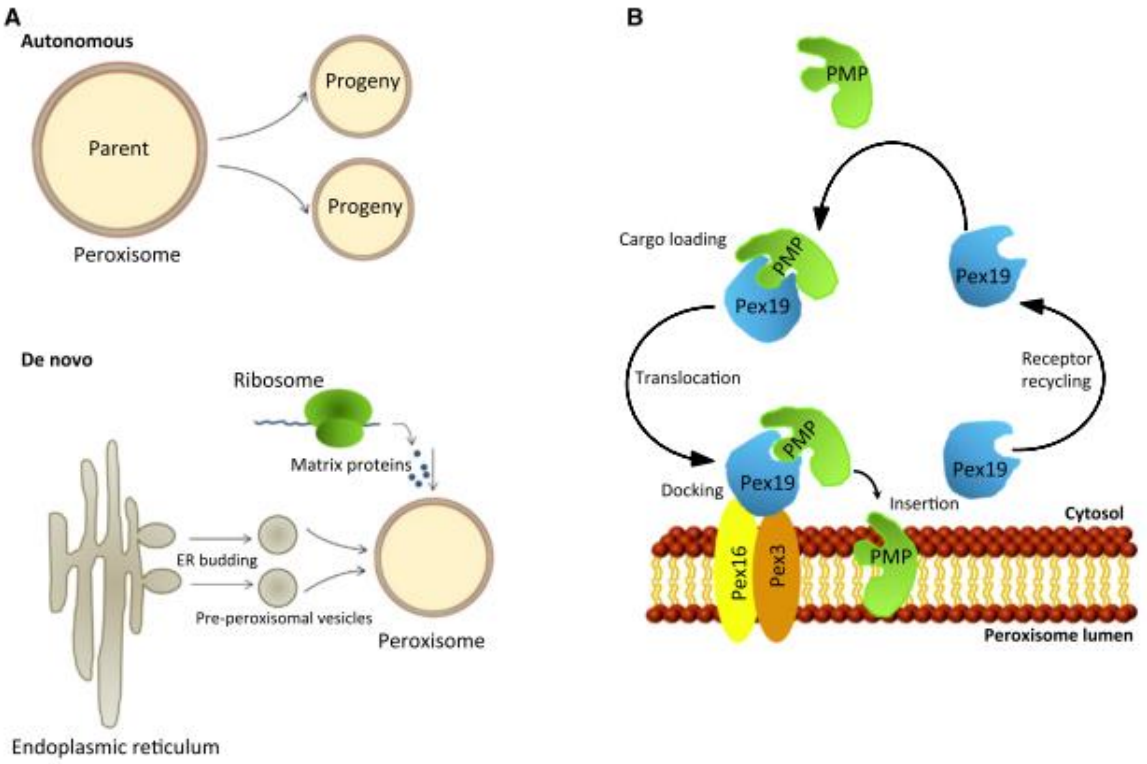

Figure 6 | Potential pathways to peroxisomal biogenesis (81). (A) Peroxisomes are generated autonomously through division of pre-existing organelles (top) or through a *de novo* process involving budding from the ER followed by import of matrix proteins (bottom). (B) Peroxisomal membrane protein import. PMPs are imported post-translationally to the peroxisomal membrane. Pex19 is a soluble chaperone that binds to PMPs and transports them to the peroxisomal membrane, where it docks with a complex containing Pex16 and Pex3. Following insertion of the PMP, PEx19 is recycled back to the cytosol.

Synthesis of peroxisomal matrix proteins occur on free ribosomes in the cytosol being then post-translationally imported into the organelle. Proteins that present one of two peroxisomal targeting signals (PTS1 and PTS2) are recognized by soluble receptors (Pex5 and Pex7, respectively), that transport them to docking sites present at the peroxisomal membrane. After recognition, the receptor-cargo complex is translocated into the luminal side of peroxisomes, cargo is released and receptors are shuttle back to the cytosol. The importer mechanism for PMPs requires a different and less characterized protein machinery that involves the cytosolic receptor/chaperone Pex19 (Figure 6). The complex formed by Pex19-PMP interacts with Pex3 and Pex16 which mediate insertion into the peroxisome membrane (88,90).

Modulation of peroxisome number and morphology

Peroxisomes react to physiological changes in their cellular environment, such as starvation, infection and cell death, adapting their abundance, morphology, distribution and enzyme content

accordingly. Peroxisomes proliferation is associated to an increased synthesis of peroxisomal enzymes. Moreover their proliferation is associated to a first elongation and posterior division. These responses of peroxisomes to alterations in their environment were verified in situations where hypolipidemic drugs or fatty acids were added as well as in cold or environmental pollutants exposition (91). It seems that, in mammalian cells, these compounds mimic the natural ligands (e.g. fatty acids, hypolipidemic fibrates) of the nuclear transcription factor peroxisome proliferator activated receptor (PPAR)-α. PPRs form heterodimers with retinoid X receptors (RXRs) and induce the transcription of peroxisomal genes involved in β-oxidation and proliferation by binding to specific DNA-sequences known as peroxisome proliferator response elements (PPRs)

Autophagy

When the requirement for peroxisomal proliferation disappears the excess of peroxisomes is removed by autophagy. Autophagy is a process regulated by ATG genes that induces sequestration and degradation of cell organelles, and other components, within lysosomes or vacuoles. There is two mechanisms for autophagy: macroautophagy and microautophagy. Macroautophagy consists in sequestering cell components within autophagosomes which then fuse with lysosomes/vacuoles, whereas in microautophagy cell components are engulfed by a lysosome/vacuole forming microautophagyc bodies (91,92).

1.3.2. Functions

Peroxisomes were identified by Christian De Duve in 1965 after isolating the organelle from rat liver and observing the co-localization between several H_2O_2-producing oxidases, as well as catalase, H_2O_2-degrading enzyme, with the organelle matrix (93). Since then, several new functions were attributed to peroxisomes. In the different organisms, peroxisomes develop a series of specialized functions: in fungi they are responsible for the biosynthesis of penicillin and degradation of methanol, in trypanosomes they perform glycolysis, in plants photorespiration and glyoxylate cycle, and in mammals they synthetize plasmalogens. Plasmalogens are etherlipids that make the neuronal myelin sheaths in the brain that, in case of loss of peroxisomal functions, is often associated with neurodegenerative processes. In mammals they are also involved in the synthesis of bile acids and docosahexanoic acid (neuromodulator), fatty acid elongation, α- and β-oxidation of certain fatty acids, metabolism of amino acids, catabolism of purines, polyamines, and mediators of inflammation such as prostaglandins and eicosanoids (83).

1. Peroxisome lipid metabolism

Peroxisomes are responsible for fatty acid β-oxidation, fatty acid α-oxidation, and ether phospholipids biosynthesis (Figure 7). In plants and fungi cells, peroxisomes are the only organelle responsible for fatty acid metabolism, although in animal cells, fatty acid oxidation also occurs through the coordination between peroxisomes and mitochondria (94). For a long time, it was though that peroxisomal β-oxidation was an auxiliary system for the mitochondrial β-oxidation pathway in case of fatty acid overload. This notion was refuted by the discovery of elevated very long chain fatty acids (VLCFAs) levels in patients with peroxisomal abnormalities, suggesting that peroxisomes have their own role in β-oxidation (95). This led to the discovery of specific substrates for both mitochondrial and peroxisomal β-oxidation (96).

The process of β-oxidation involves four main reactions: 1) dehydrogenation, 2) hydration, 3) dehydrogenation, and 4) thiolytic cleavage (80). In each cycle fatty acids are shortened by two carbons atoms which are released as acetyl-coenzyme A (acetyl-CoA). However, β-oxidation cannot be completed in peroxisomes being acyl-CoA esters shuttled to mitochondria for further oxidation (95). Peroxisomal β-oxidation is a heat-generating process contributing for thermogenesis. In the 1st phase of oxidation, electrons released from FAD-linked oxidases are donated to an oxygen producing H_2O_2, and in the 2nd phase electrons are taken by NAD^+, that has to be reoxidized in mitochondria (Figure 7) (97).

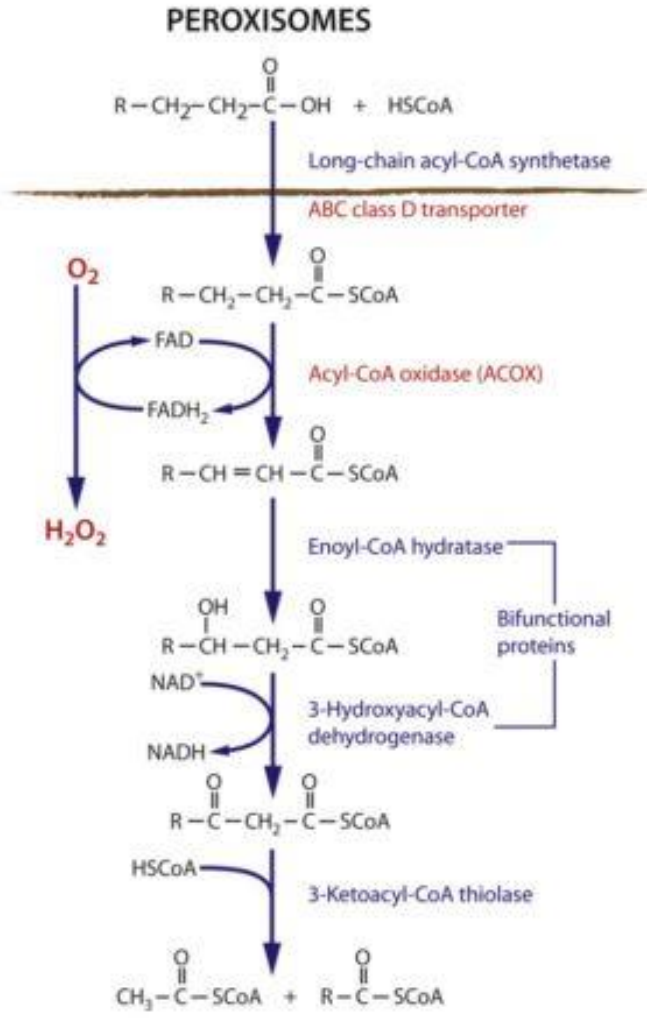

Figure 7 | Peroxisomal fatty acid β-oxidation pathways (Adapted from Camões el al. 2014) (98).

2. ROS metabolism in peroxisomes

Reactive oxygen species (ROS) and reactive nitrogen species (RNS) consist in by-products of metabolic reactions, like H_2O_2 produced by peroxisomes. To counterbalance the production of negative molecules and protect cells, peroxisomes also have mechanisms to counteract oxidative stress and maintain redox homeostasis (99). Catalase, alongside with other enzymes, is an anti-oxidant enzyme present in the matrix of peroxisomes that allow peroxisomes to participate in cell response to stress. Catalase acts by converting H_2O_2 into water and O_2, additionally catalase also metabolize ethanol, methanol, phenols and nitrites (99,100). ROS participate in several cell signalling pathways but overproduction can induce oxidative modifications of different molecules, such as proteins, lipids and nucleic acids, and under oxidative stress conditions can lead to diverse pathological conditions (97).

1.3.3. Peroxisomes in health and disease

Given the important roles of peroxisomes in cellular metabolism, their dysfunction can lead to severe neurological and developmental disorders (101)

The peroxisomal disorders represent a group of genetic diseases associated to the impairment of one or more peroxisomal functions. They are subdivided into three subgroups: 1) the peroxisome biogenesis disorders; 2) the single peroxisomal enzyme deficiencies; 3) the single peroxisomal substrate transport deficiencies (84). The discovery of these different types of disorders associated to peroxisomes helped in the sorting of essential peroxisomal components in health and disease. The important role of peroxisomes in β-oxidation was discover after the identification of a patient where VLCFA accumulate in cells due to a peroxisomal dysfunction. This pathology was named as Zellweger syndrome, and it is characterized by the absence of morphologically identifiable peroxisomes. In patients with this disorder it was also found a deficiency of plasmogens, phospholypids important for neural tissue and also present in erythrocytes (85).

Peroxisomes are also important for ROS metabolism, as indicated previously. Any dysfunction in ROS metabolism can also induce the onset of several neurodegenerative as Parkinson's Disease, Alzheimer's disease, as well as cancer and ageing (96).

As already described in the section 1.2 of introduction, peroxisomes are also associated to the coordination of antiviral signalling with mitochondria. Moreover, it was also detected that peroxisomal morphology suffers some alteration. Dixiet et al. (2010) described that reovirus infection induced peroxisomal aggregation and the formation of peroxisomal tubules. These alterations were correlated with the peroxisomal-MAVS signalling activation during infection (67). Another example is the use of peroxisomes as replication site. In infections caused by members of the tombusvirus family it was detected that p33, a member of the replication complex, associated with plant peroxisomes (102). Other viruses like HIV and influenza express proteins that were found at peroxisomes (103).

Thus, peroxisomes are essential organelles for cells having specific and important functions. They coordinate with others organelles, like mitochondria, ER and lipid droplets various signalling cascades. Lately, peroxisomes have been associated with viral-host interactions, however their function during infection is still elusive.

II. Objectives

II. Objectives

HCV is a major human viral pathogen that infects hepatocytes causing liver cirrhosis, chronic hepatitis and hepatocellular carcinoma. Since HCV discover in 1989 a lot has been learned about its life cycle and host-interaction, however several pathways have to be better elucidated, such as cell recognition and entry, factors that regulate replication and translation, or even virion assembly. HCV is highly dependent of cellular lipid metabolism - virions incorporate lipids in their structure and associate with lipoproteins what may increase HCV infectivity.

Until recently, peroxisomes were thought to be an auxiliary organelle to mitochondrial pathways in cellular metabolism. However, the existence of pathologies that occur due to a malfunction or inexistence of peroxisomes in cells rise the importance of peroxisomes in health and disease. Additionally, recent studies showed that peroxisomes are also involved in the coordination of the cellular antiviral response.

MAVS is a protein adaptor in the antiviral pathway activated by RLRs. MAVS was first described at mitochondria and was recently found to be also localized at peroxisomes. Both organelles coordinate MAVS pathway during viral infection acting differently but in a complementing way.

The main objective of this project is to characterize the importance of peroxisomes in antiviral immunity against HCV. For this, I will investigate the effect of NS3/4A, a protease that allows HCV evasion, in HCV evasion from the cellular antiviral defence coordinated by peroxisomal MAVS. It was already described that this complex target MAVS at mitochondria, however nothing is known concerning it targeting of peroxisomal.

To achieve this objective the following specific aims were proposed:

1. Development of a MAVS construct that is targeted exclusively to peroxisomes and contains the recognition site for HCV NS3/4A cleavage;

2. Examine the localization at peroxisomes of the construct developed;

3. Identify the effect of NS3/4A over the peroxisomal MAVS;

4. Evaluate if MAVS cleavage by NS3/4A impairs the cellular antiviral response.

III. Material and Methods

III. Material and Methods

3.1. Material

3.1.1. Bacterial Strains

- E.coli XL-Blue, Stratagene

3.1.2. Vectors

- pEGFP-C1
- pCMV-C3

3.1.3. Plasmids

- pEGFP-C1-MAVS-WT
- pCMV-C3-MAVS-WT
- pCMV-C3-MAVS511Pex
- pEGFP-C1-NS3/4A
- pEGFP-C1-RIG-I-CARD

3.1.4. Chemicals and reagents

- Acetic Acid, Merck Millipore
- Acrilamide, Fisher Scientific
- Agar, Formedium
- Agarose, Roth
- Ammonium Persulfate (APS), Sigma
- Bovine serum albumin (BSA), NZYTech
- Bromophenol Blue, Sigma
- Chloroform, Merck Millipore
- Dimetilsulfóxido (DMSO), EMD Chemicals
- Dithiothreitol (DTT), Sigma
- Ethanol, Merck Millipore
- Ethylenediaminetetraacetic acid (EDTA), Sigma
- Ethidium Bromide, Sigma
- Foy, Schwarz-Pharma
- Glucose, Fluka
- Glycerol, Roth
- Glycine, Fisher Scientific
- Hydrochloric acid (HCl), Merck Millipore
- Isopropanol, Merck Millipore

- Kanamycin (Kan), Sigma
- Lysogeny broth (LB), Fisher Scientific
- Methanol, Merck Millipore
- Midori Green Advance, Nippon Genetics
- Milk, Néstle
- Mowiol, Applichem
- N-propyl-gallacte, Fluka
- Paraformaldehyde (PFA), Sigma
- Potassium chloride (KCl), Sigma
- Penicillin/ Streptomycin, Labclinics
- Phenylmethylsulfonyl fluoride (PMSF), Sigma
- RNAse free water, Fisher Scientific
- Sodium chloride (NaCl), Sigma
- Sodium dodecyl sulfate (SDS), Sigma
- Sodium Deoxylacholat, Sigma
- Sodium phosphate (NaHPO4), Sigma
- iTaq™ Universal SYBR® Green Supermix, BioRad
- Tetramethylethylenediamine (TEMED), Fluka
- Trifast, PeqLab
- Tris, Fischer Scientific
- Trasylol, Bayer
- Triton, Sigma
- Tween-20, Sigma
- β-Mercaptoethanol, Sigma

3.1.5. Solutions and buffers

- **BSA 1%**: 2% BSA diluted in 1x PBS
- **Blotting Buffer**: 0.05 M Tris, 0.4 M Glicina, 0.05% SDS, 20% Methanol
- **LB/Agar**: 2 g agar, 20 g LB, 1000 mL ddH_2O
- **Lysis Buffer**: 25 mM Tris-HCl pH 8, 50 mM NaCl, 0.5% Sodium Deoxylacholat, 1.5 mM Triton X-100
    - Add protease inhibitors before use: 0.01 mM Foy, 0,25 (v/v) Trosylol, 0,1 mM PMSF
- **Loading buffer**: 1 M Tris pH 6.80, 10% Glycerol, 1 M DTT, 20% SDS, β-Mercaptoethanol, 0.1% Bromophenol Blue
- **Mounting Medium**
    - **N-propyl-Gallat**: 2.5% (w/v) n-propyl-gallat; 50% glycerol, in PBS
    - **Mowiol**: 12 g Mowiol 4-88, 20 mL Glycerol, 40 mL PBS
    - **Mounting medium**: 3:1 mixture Mowiol with n-propyl-gallate
- **PFA 4 %**: 20 g PFA in 450 mL ddH2O, 4 drops 1 M NaOH, 50 mL 10x PBS
- **1x PBS**: 1.39 M NaCl, 80 mM $NaHPO_4$, 0.0268 M KCl, 0.0147 M KH_2PO_4 pH 7.36, prepared from 10x PBS diluted in ddH_2O
- **Running Buffer 1x**: 250 mM Tris, 1.9 M Glycin, 1% SDS
- **Solution I**: 50 mM glucose, 25 mM Tris-HCl pH 8, 10 mM EDTA
- **Solution II**: 0,2 M NaOH, 1% SDS
- **Solution III**: 60 mL 5 M KAc, 11.5 mL glacial acetic acid, 28.5 mL ddH_2O

- **Stripping Solution**: 62.5 mM Tris-HCl pH 6, 2% SDS, 100 mM β-Mercaptoethanol
- **1x TAE**: 0.04 M Tris, 0.02 M Acetic Acid, 1 mM EDTA pH 8, prepared from TAE 50x diluted in ddH_2O
- **1x TBS-T**: 100 mM Tris pH 8, 1,5 M NaCl, 0,05% Tween20, prepared from 10x TBS-T diluted in ddH_2O
- **0,2%Triton X-100**: 0.2% Tx-100 in 1x PBS

3.1.6. Kits

- Clarity Western ECL Substrate, BioRad
- NucleoBond Xtra Midi, Macherey-Nagel
- NucleoSpin Plasmid, Macherey-Nagel
- NucleoSpin Gel and PCR clean-up, Macherey-Nagel
- 6x Orange DNA Loading Dye, Fermentas
- KOD Hot Start DNA Polymerase, Novagen
- Neon Transfection System Kit, Invitrogen

3.1.7. Enzymes and Markers

Enzymes

Table 2 | Detailed information about enzymes.

Enzyme	Sequence (5'- 3')	Buffer	Manufacture
EcoRI	G|AATTC	NeBuffer 2	New England BioLabs
HindIII	A|AGCTT		
KpnI	GGTAC|C		
XhoI	C|TCGAG		
T4 DNA Ligase	-	10x T4 DNA Ligase Reaction Buffer	
M-MuLV Reverse Transcriptase	-	10x M-MuL V Reverse transcription Buffer	

Markers

- O'GeneRuler DNA Ladder Mix, Fermentas
- NZYColour Protein Marker II, NZYtech

3.1.8. Membranes

- Protran BA85 Nitrocellulose Blotting Membrane, GE Healthcare

3.1.9. Equipment

- My Cycler Thermal Cycler, BioRad
- PowerPac HC High-Current Power Supply, BioRad
- Mini-PROTEAN Tetra Cell and blotting module, BioRad
- Electrophoresis Power Suply EPS 3501 XL Power Supply, GE Healthcare
- Centrifuge Heraeus Pico and Fresco 17, Thermo Scientific
- Molecular Imager GelDoc, BioRad

- Electromagnetic agitator VMS-C7, VWR
- UV-3100 PC Spectrophotometer, VWR
- Incubation shaker CERTOMAT BS-1, Sartorius
- Olympus IX81 microscope, Olympus Optical
- Leica TCS SP5 confocal microscope, Leica Microsystems
- *GS-710 calibrated Imaging Densitometer, BioRad*
- Vaccum gas pump, VWR
- Shaker, Mini-Rocker PMR-30, Grant Bio
- Water Bath VW36, VWR
- Pipettes Eppendorf Research, Eppendorf
- Basic pH meter PB-11, Sartorius
- Vertical Laminar Flow Hood HERASafe, Heraeus
- CO2 incubator MCO-17AIC, Sanyo
- Inverted microscope Leica DM IL LED, Leica
- Analytical balance VWR, Sartorius
- Thermomixer Comfort 1.5, Eppendorf
- Neon Transfection System, Invitrogen
- 7500 Real-Time PCR System, Applied Biosystems

3.1.10. Databases and Software

- Image Lab, BioRad
- *Quantity One 1-D Analysis Software, BioRad*
- *LAS AF LITE, Leica*
- *Basic Local Alignment Search (BLAST) Tool, National Center for Biotechnology Information (NCBI)*
- FinchTV 1.4.0 program, Geospiza
- Excel, Microsoft
- Serial Cloner

3.1.11. Cells strain

- MEF KO MAVS (kindly provided by Dr. Kagan (Harvard Medical School, USA))

3.1.12. Culture cell solutions and plates

- Dulbecco's Modified Eagle Medium (DMEM) High Glucose w/ L-Glutamine w/o Sodium Pyruvate, BioWest
- Dulbecco's Phosphate Buffered Saline w/o Calcium w/o Magnesium, BioWest
- Trypsin-EDTA 1X in PBS w/o Calcium w/o Magnesium w/o Phenol Red, BioWest
- Fetal Bovine Serum (FBS), qualified, E.U.-approved, South America origin, Gibco
- Opti-MEM Reduced-Serum Medium (1x) liquid, Gibco

3.1.13. Transfection Reagents

- Lipofectamine 3000 Transfection Reagent, Invitrogen

3.1.14. Primers

Table 3 | List of primers used.

Primer	Sequence (5'-3')	Manufacture
Primer FW 1	CC CAA GCT TGG ATG CCG TTT GCT GAA GAC	Eurofins
Primer RV 2	C ATG CAC AAT GGG CCT GTG GCA TGC	
Primer FW 3	GC CAC AGG CCC ATT GTG CAT GCA TTT GCC	
Primer RV 4	G GGGTAC CTC GAG TTA AGA TTT TGC TGA GG	
Primer FW Ns3	C CC CAA GCT TGG ATG GCG CCC ATC ACC	
Primer RV Ns3	G GGG TAC CTC GAG TTA GCA CTC TTC CAT CTC	
Oligo-dT primer	-	
Viperin mouse Fw	TGTGAGCATAGTGAGCAATGG	
Viperin mouse RV	TGTCGCAGGAGATAGCAAGA	
IRF 1 mouse FW	GGTCAGGACTTGGATATGGAA	
IRF 1 mouse RV	AGTGGTGCTATCTGGTATAATGT	
GAPDH mouse FW	AGTATGTCGTGGAGTCTA	
GAPDH mouse RV	CAATCTTGAGTGAGTTGTC	

3.1.15. Antibodies

Table 4 | Information of primary and secondary antibodies.

Antibody	Species	Production	Dilution		Company	Code
			IMF	WB		
Primary Antibody						
Pex14	Rabbit		1:1400	-	Provided by Dr. Crane (Eskitis Institut, Australia)	
PMP70	mouse	monoclonal	1:200	-	Sigma	SAB4200181
TOM20	mouse	monoclonal	1:100	-	BD Biosciences	612278
	rabbit	polyclonal	1:100	-	Sigma	HPA011562
Myc	rabbit	monoclonal	1:200	1:1000	Cell Signaling	2278
	mouse	monoclonal	1:200	-	Santa Cruz Biotecnhology, Inc	sc-40
MAVS	mouse	monoclonal	-	1:2000	Santa Cruz Biotechnology, Inc.	sc-166583
GFP	rabbit	monoclonal	1:200	1:4000	Invitrogen - Molecular Probles	polyclonal
Tubulin	mouse	monoclonal	-	1:4000	Sigma	T9026
IRF-1	rabbit	polyclonal	-	1.1000	Santa Cruz Biotecnhology, Inc.	sc-640
RIG-I	mouse	-	-	1:500	Provided by Dr. Weber (Institute of Virology, Germany)	
Viperin	mouse	-	-	1:500	Provided by Dr. Cresswell (Yale University, USA)	
Flag	rabbit	monoclonal	1:750	1:1000	Sigma	F7425

Secondary Antibody						
Alexa 488	rabbit	-	1:400	-	Invitrogen - Molecular Probles	A21206
	mouse		1:400	-	Invitrogen - Molecular Probles	A21202
Tritc	rabbit		1:100	-	Jackson Imunoresearch	111-026-003
	mouse		1:100	-	Jackson Imunoresearch	715-025-150
Alexa 647	rabbit		1:150	-	Provided by Dra. Carvalho (CNC, Portugal)	
HRP	rabbit		-	1:5000	BioRad	170-6515
HRP	mouse		-	1:5000	BioRad	170-6516
HoechstDye (1mg/mL)	-		1:2000	-	Jackson Imunoresearch	711-475-152

3.2. Methods

3.2.1. Cloning

Amplification of MAVS511Pex and NS3/4A

MAVS-511-Pex

For the development of this work, we had to develop a specific construct named MAVS511Pex. This construct consists in the sequence of MAVS that encodes the first 511 aa and a transmembrane domain from Pex13 that redirects the protein for peroxisomes. The development of this clone was possible due to a successive set of amplifications in which templates were the MAVS-WT and MAVS-Pex described in Dixit et al. (2010) and kindly provided by Dr. Kagan (Harvard Medical School, USA). Thus, we first amplified the sequence that encodes the first 511 aa from MAVS-WT using the forward primer 5' CC CAA GCT TGG ATG CCG TTT GCT GAA GAC 3' (primer 1) and the reverse primer 5' C ATG CAC AAT GGG CCT GTG GCA TGC CAC 3' (primer 2). In parallel, we amplified the sequence of Pex13 transmembrane domain present in MAVS-Pex using the forward primer 5' GC CAC AGG CCC ATT GTG CAT GCA TTT GCC 3' (primer 3) and the primer reverse 5' G GGGTAC CTC GAG TTA AGA TTT TGC TGA GG 3' (primer 4). After purifying the reaction products of each PCR, both were used as a template for the last reaction, together with primer 1 and primer 4, resulting in MAVS511Pex sequence. These two last primers were designed with restriction sites that allowed the construct insertion into the pCMV-3C vector. The PCR conditions for each reaction are presented in Table 5.

Table 5 | PCR conditions of MAVS-511-Pex insert cloning

Steps	PCR 1			PCR 2			PCR 3		
Initialization	1x	95°C	2:00	1x	95C	2:00	1x	95°C	2:00
Denaturation	4x	94°C	0:30	5x	94°C	0:30	5x	94°C	0:30
Annealing		50°C	0:40		43°C	0:30		52°C	0:30
Extension		70°C	1:40		70°C	0:30		70°C	3:00
Denaturation	30x	94°C	0:30	25x	94°C	0:30	25x	94°C	0:30
Annealing		65°C	0:30		65°C	0:30		65°C	0:30
Extension		70°C	1:40		70°C	0:30		70°C	3:00
Elongation	1x	70°C	10:00	1x	70°C	10:00	1x	70°C	10:00
Final Hold	4°C		∞	4°C		∞	4°C		∞

NS3/4A

NS3/4A was kindly provided by Dr. Eliane Meurs (Institut Pasteur, France), however for this work it had to be inserted in a pEGFP-C1 vector. For this, primers were design to contain the appropriate restriction sites, primer forward 5' C CC CAA GCT TGG ATG GCG CCC ATC ACC 3' and primer reverse 5' G GGG TAC CTC GAG TTA GCA CTC TTC CAT CTC 3'. The NS3/4A was amplified using the program detailed in table 6.

Table 6 | PCR conditions of NS3/4A cloning.

Steps	PCR –NS3/4A		
Initialization	1x	95°C	2:00
Denaturation	4x	94°C	0:30
Annealing		48°C	0:30
Extension		70°C	2:00
Denaturation	25x	94°C	0:30
Annealing		65°C	0:30
Extension		70°C	2:00
Elongation	1x	70°C	0:30
Final Hold	4°C		∞

All the reactions were carried in a thermal cycler (BioRad) using the KOD Hot Start DNA Polymerase (Novagen).

DNA electrophoresis and isolation

In the end of each PCR reaction the products of interest were isolated by DNA electrophoresis which ran in a 0.7% agarose gel in 1x TAE, stained with 0.5 µg/mL of ethidium bromide, at 70 V for

1 hour and 30 min in 1x TAE running buffer. To follow sample's running, they were mixed with a loading dye (Fermentas) and a DNA maker (Fermentas) was loaded to allow sizing and quantification. Photos were taken using the GelDoc (BioRad) and treated with the Image Lab (BioRad) program. The bands of interest were excised under the UV light with a scalpel. They were isolated and purified with NucleoSpin Gel and PCR clean-up (Macherey-Nagel) as the protocol indicates.

Restriction digestion and ligation

Inserts (MAVS511Pex and NS3/4A) and vectors (pEGFP-C1) were digested with the restriction enzymes Hind III, Kpn I (New England Biolabs) in the Nebuffer 2 (New England Biolabs) at 37°C for 3 hours.

The fragments were then separated by DNA electrophoresis as described above with a 1% agarose gel in 1x TAE, at 75 V for 1 hour and purified with the same kit. In the end, samples were quantified with the program *Image lab* (BioRad).

The vector-insert ligation was performed in a molecular ratio of 1:3 (Figure 8) and both were incubated with a T4 DNA ligase in NEBuffer U (New England Biolabs) at 16°C overnight.

$$Mass\ insert\ (ng) = \frac{mass\ vector\ (ng) \times length\ insert\ (kb)}{length\ insert\ (kb)} \times 3$$

Figure 8 | Formula used to calculate insert quantity for ligation protocol

Bacterial transformation

For bacterial transformation, 50 µL of competent E.coli XL Blue were mixed with 5 µL of ligation DNA and incubated for 30 minutes on ice. After the heat shock at 42°C for 90 seconds and 3 minutes on ice, bacteria recuperated in 950 µL of LB for 45 minutes at 37°C and at 200rcf. Then, bacterial suspension centrifuged for 1 minute at 1700rcf and some supernatant was discarded. The pellet was resuspended in the remaining supernatant and glass beads helped to spread bacterias in LB/agar/kanamycin plates. An incubation at 37°C overnight followed. The protocol was done under a sterile environment and the appropriate controls were used.

Colony selection

Several test colonies were inoculated in 3 mL of LB medium (with kanamycin) for 16 hours at 37°C with shaking (200rcf). Plasmid isolation was accomplished through a miniprep protocol based in alkaline lysis. 1.5mL of each bacterial suspension was centrifuged at 12000 rcf during 2 minutes. The pellet was lysed in 100 µL of cold solution I and vortexed vigorously before desnaturation in 200 µL of solution II. Then, it was inverted 5 times and incubated for 5 minutes with 150 µL of cold solution III before being centrifuged at 17000 rcf for 10 minutes at 4°C. To precipitate and purify the DNA, the supernatant was discarded and 1 mL of ethanol was added. Samples were centrifuged at 17000 rcf during 5 minutes at 4°C and the supernatant was once again discarded. After drying the pellet at room temperature, it was rehydrated in 50 µL of water with RNase.

To define which colonies were positive, two restriction analysis with the same conditions as described above were performed. A positive colony was selected and purified using the NucleoSpin Plasmid kit (Macherey-Nagel). The manufacture's protocol was followed.

To insert MAVS511Pex in the pCMV-3C vector it was necessary to do an enzymatic restriction in the GFP-MAVS511Pex and in the pCMV-3C vector with HindIII and XhoI restriction enzymes in NeBuffer2 for 3 hours at 37°C. Afterwards, the previously described procedure was followed from ligation up to the purification.

Sequencing

To confirm the sequence of each construct, they were sent for sequencing at Eurofins MWG Operon (Germany). For that, suspension cultures in 4 mL of LB medium (with kanamycin) were prepared from each positive colonies of pEGFP-C1-MAVS511Pex, pCMV-3C-MAVS511Pex, pEGFP-C1NS3/4A. After incubating for 16h at 37°C with shaking (200rcf), the DNA was isolated using the protocol provided by NucleoSpin Plasmid, Macherey-Nagel. After quantification, the samples were sent to be sequenced. The sequences were analysed with the FinchTV 1.4.0 program (Geospiza) and compared with the original sequences using the Basic Local Alignment Search (BLAST) Tool from National Center for Biotechnology Information (NCBI).

After sequence confirmation, high quality plasmids were grown in high quantity for transfection. 3mL of each culture were add to 200 mL of LB medium (with kanamycin) and incubated for 16 hours at 37°C with shaking (200rcf). Then, the plasmids were purified following the NucleoBond® Xtra Midi (Macherey-Nagel) protocol.

3.2.2. Cell culture

Cell Maintenance

The cells chosen for this project were the Mouse Embryonic Fibroblasts (MEF) cells with a knock-out of MAVS protein (MEF KO MAVS). These cells were kindly provided by Dr. Kagan (Harvard Medical School, Boston) and were used for all the experiments presented.

MEF KO MAVS were routinely cultured in DMEM high glucose (4,5 g/L) supplemented with 10% FBS, 100U/mL penicillin and streptomycin at 37°C in a humidified atmosphere containing 5% CO_2.

After reaching the desired confluence, cells were passed and split twice a week. Confluent cells were washed with PBS and after incubating 1 minute with 2 mL trypsin-EDTA at 37°C and 5% CO_2 they were harvested with 6 mL of cell culture medium and centrifuged at 1000 rcf for 3 minutes at room temperature. Upon resuspention of the cell pellet in 10 mL of cell culture medium, cells were seeded in a 1:10 dilution (≈10^5 cells/mL). Cells were routinely grown on 10øcm culture dishes. For the immunofluorescence studies, cells were seeded on 6øcm dishes with 5 round 18ømm glass coverslips and for the immunoblotting and RT-qPCR experiments 6 well plates were used.

Cell storage, freezing and thawing

Cells stocks were kept in liquid nitrogen for cryopreservation. Stocks were prepared from confluent cells as described above and resuspended in freezing medium (DMEM supplemented with 20% FBS and 10% DMSO). Cells were preserved in cryovials aliquots of 1 mL and frozen overnight in -80° before being placed in the liquid nitrogen tank.

When needed, cells were thawed through resuspention with pre-warmed culture medium and seeded in a 10øcm culture dishes. After cell adhesion (≈ 5 hours) the medium was changed to remove cell debris and DMSO.

3.2.3. Transfection methods

Lipofectamine 3000

Two reactions were prepared: first, 8 µL Lipofectamine 3000 reagent was diluted in 250 µL Opti-Mem and in a second one DNA was diluted with 8 µL P3000 in 250 µL Opti-Mem. After 5 minutes of incubation at room temperature the second reaction was added to the first and incubated for more 5 minutes in the same conditions. Then, the DNA/reagent complex was added drop-wise to

6øcm culture dishes and incubated for 4 hours at 37°C after which the cells were washed with PBS and incubated for more 24 hours in fresh culture medium. Different quantities of DNA were used, 6µg of Myc-MAVS-511-Pex, 6 µg of Myc-MAVSWt and/or 8 µg of Gfp-NS3/4A.

Golden Needle Microporation

Cells at a density of $5x10^6$ were resuspended in *Resuspension Buffer R*. After adding 10 µg of DNA to the cell suspension, cells were microporated using the Neon Transfection System with 1 pulse in 3 mL of *Electrolytic Buffer E* with a 10 µL *Neon Tips*. Microporation pulse conditions were 1350 V for 30 seconds. Cells were then incubated in 6øcm culture dishes with 10mL of culture medium with FBS and without antibiotics for 6 hours at 37°C before changing to complete medium.

3.2.4. Immunofluorescence

Cells grown in glass coverslips were washed three times with PBS before being fixated for 20 minutes with 4% para-formaldehyde, permeabilized with 0,2% Triton X-100 for 10 minutes, and blocked with 1% BSA for 10 minutes. Cells were stained with 30 µL of the primary antibody as well as with the secondary antibody for 1 hour in a humid environment, protected from the light. Finally, coverslips were incubated with 30 µL of Hoechst dye for 2 minutes. All the incubations were done at room temperature and, between each step the cells were washed three times with PBS. Coverslips were washed in ddH_2O, mounted in glass slides with mounting medium and dried for at least 24 hours. Glass slides were stored at 4°C.

For these experiments, the cells were observed with an Olympus IX-81 inverted (Olympus Opical Co.) microscope, 100x/1.40 oil objective (Olympus Optical) equipped with the appropriate filter combinations and a 100x objective (Plan-Neofluar, 100x/1.35 oil objective). Confocal photos were acquired with a Leica TCS SP5 confocal microscope, Plan-Apochromat 63x and 100x/1.40 oil objectives (Leica), using the *LAS AF LITE* (*Leica*). The lasers used were 488 nm Argon-ion laser, 561 nm DPSS laser and 642 nm HeNe for samples stained with Alexa Fluor 488 dye, TRITC dye and Alexa 647 dyed, respectively.

3.2.5. Immunoblotting

Lysis and harvesting

Cells were seeded 48 hours in 6øcm dishes and transfected 24 hours before being washed three times with PBS. Then, after being harvested with 200 µL of lysis buffer and a scrapper, the samples were resuspended 20 times with a 26G syringe. An incubation for 30 minutes at 4°C with

head-rotation was performed and the samples centrifuged for 15 minutes at 13 000 rcf in 4°C. The collected supernatant was stored at -20°C.

For measurement of the samples' protein concentration, the Bradford protein assay was performed. The bradford reagent was diluted (1:5) with ddH_2O and a series of BSA standards were prepared in duplicate with known protein concentrations (1 µg/µL BSA diluted in 1 M NAOH: 0.01-0.11 µg/µL). To measure the samples 0,3 µL of protein extract was diluted in 1 M NAOH. After adding 1 mL of Bradford, the dilutions were incubated for 15 minutes at room temperature. After, standards and the samples absorbance were measured at 595 nm with a Spectrophotometer (VWR), a standard curve was draw in Excel program (Microsoft) and samples concentration was calculated.

Protein electrophoresis and blotting

50 µg of protein extracts diluted in 5x loading buffer incubated for 15 minutes at 65°C. Samples were loaded alongside with a pre-stained protein marker (Nzytech) in mini handcast gels prepared with 7% polyacrylamide resolving gel and 4% stacking gel. The gel chamber was filled with running buffer and electrophoresis was conducted in running buffer for 1 hour and 30 minutes at 150 V. Bromophenol blue presented in the loading buffer allowed sample running visualization.

After protein's separation, the gel was assembled with a nitrocellulose membrane and Whatman filter paper in a mini trans-blot system. After equilibrating all the components in transfer buffer, they were set in a specific order: foam pad, filter paper, gel, membrane, filter paper and foam pad inside the cassette. To ensure the transfer, air bubbles that could had form were taken by pressing all the components. The chamber was filled with transfer buffer and the blotting was conducted at 0.4 A for 2 hours on ice.

Immunodetection

After blotting, the membrane was washed to take out methanol residue before being blocked with 5% low fat powder milk in TBS-T for 50 minutes. Membrane staining was accomplish by incubation with a primary antibody, for 1 hour to 3 hours depending on the antibody, and a secondary antibody, for 1 hour, both at room temperature with shaking. Between incubations, three washing steps of 10 minutes each with TBS-T were performed.

For enhanced chemiluminescence detection, membrane was incubated with a chemiluminescent substrate solution, a mixture 1:1 of luminol and peroxide from the *Clarity Western ECL Substrate kit (BioRad)*, for approximately 3 minutes before exposing to a photographic film for 30 seconds to 10 minutes. Exposition, fixation and development occurred in a light protected environment. Photos were taken with a Densitometer (BioRad) and analysed with the Quantity One (BioRad) software.

3.2.6. Reverse transcriptase - quantitative Polymerase Chain Reaction

RNA extraction

Cells were washed with PBS and lysed by incubating 5 minutes at room temperature with 500 µL Trifast/Trizol before collection. 100 µL of chloroform were added and the samples were shaken vigorously for 15 seconds and incubated for more 5 minutes at room temperature. Following a centrifugation for 15 minutes at 12000 rcf, the upper aqueous phase containing RNA was extracted. RNA was incubate with 250 µL of isopropanol for 10 minutes. After centrifugation for 15 minutes at 12000 rcf, the supernatant was removed. The pellet was washed two times with 500 µL of 75% ethanol and centrifuged for 5 minutes at maximum speed. After removing the ethanol, the pellet dried for 10 minutes before being resuspended with 30 µL of RNAse free water.

The RNA concentration was measured with Nanodrop after being dissolved at 55°C and RNA quality was also assessed by electrophoresis. The RNA mixed with loading dye ran in a 1% agarose gel stained with Midori Green for 1 hour at 100V.

cDNA synthesis

cDNA synthesis was accomplished by mixing 2µg RNA with a master mix of 280 pmol oligo-dT primer, 166 µM dNTPs, 1x M-MuL V Reverse transcriptase buffer, 100 U M-MuL V Reverse transcriptase, 20 U RNAse inhibitor and RNAse free water . This mixture incubated for 10 minutes at room temperature. Then, cDNA was synthesised for 90 minutes at 42°C and the enzyme was inactivated for 20 minutes at 65°C.

Real-time Quantitative Polymerase Chain Reaction

The primer sequences used for quantification of IRF1 were 5’ GGTCAGGACTTGGATATGGAA 3’ and 5’ AGTGGTGCTATCTGGTATAATGT 3’, for viperin were 5’ TGTGAGCATAGTGAGCAATGG 3’ and 5’ TGTCGCAGGAGATAGCAAGA 3’ and for GAPDH were 5’ AGTATGTCGTGGAGTCTA 3’ and 5’

CAATCTTGAGTGAGTTGTC 3'. All sequences were designed using the Beacon Desigen 7 (Premier Biosoft) and GAPDH was used as a reference gene. The real-time polymerase chain reaction mix was prepared with 2 µL of 1:10 diluted synthesized cDNA, 10 µL of 2× iTaq SYBR Green Master Mix (BioRad) and each primer was added to a final concentration of 250 nM for a total volume of 20 µL. Using the 7500 Real-Time PCR System (Applied Biosystems), the reaction initiated by heating at 95°C for 3 min, followed by 40 cycles of a 12 seconds denaturation step at 95°C and a 30 seconds annealing/elongation step at 60°C. The fluorescence was measured after the extension step, using the Applied Biosystems software. After the thermocycling reaction, the melting step was performed with slow heating, starting at 60°C and with a rate of 1%, up to 95°C, with continuous measurement of fluorescence. Data analysis was performed using the $2-\Delta\Delta CT$ method.

3.2.7. Statistics

For the quantitive analysis of IRF1 and viperin mRNA expression three independent experiments were done. Statistical analysis was performed in Graph Pad Prism 5. Data represent the means ± standard error mean (SEM). To determine the statistical significance between the experimental groups the one-way ANOVA followed by Bonferroni's multiple comparison tests were applied. P values of ≤ 0.05 were considered as significant.

IV. Results

IV. Results

4.1. Myc-MAVS511Pex and GFP-NS3/4A plasmids contruction

MAVS was first discovered to localize at mitochondria and more recently Dixit et al. (2010) have shown that it is also present at peroxisomes (67). In both organelles, MAVS acts as a signalling transducer in the immune response against infection triggered by the activation of RIG-I and/or MDA5 upon recognition of viral genomes (63–65,67,71). Furthermore, it was also found that the presence of MAVS in both organelles has different but complementing functions: peroxisomal MAVS induces a rapid but short-termed interferon-indendent response, which contrasts with the delayed kinetics and interferon-dependent response by the mitochondrial MAVS pathway (67).

We have received specific constructs from Kagan's laboratory (Harvard Medical School, USA) in which the MAVS localization motif was replaced with a set of domains that redirect the protein to peroxisomes or mitochondria (67). During the process of construction of these plasmids, the Cys-508 that is recognized by HCV NS3/4A was deleted (47). To study the possible effect of NS3/4A in peroxisomal MAVS, the plasmid encoding for the peroxisomal MAVS had, hence, to be modified and was altered so that the Cys-508 was re-introduced. Thus, we had to do a series of PCRs using MAVS-WT (also kindly provided by Dr. Kagan) and MAVS-Pex as templates. We started by amplifying the MAVS-WT sequence that encodes the first 511 aa. In parallel, a second PCR using the MAVS-PEX was performed in order to amplify the sequence that encodes the transmembrane domain of Pex13. Lastly, both PCR products were combined as template of the final PCR reaction resulting in MAVS511Pex construct (Figure 9, for further details on the reactions please see section 3.2.1). MAVS511Pex corresponds to the MAVS-Pex described by Dixit et al. (2010), with the extra original sequence between aa 500 and 511, necessary for NS3/4A cleavage (Figure 10A). This construct was developed with the necessary restriction sites in order to be inserted in the pCMV-3C (Figure 10B) and be express fused to a Myc-tag.

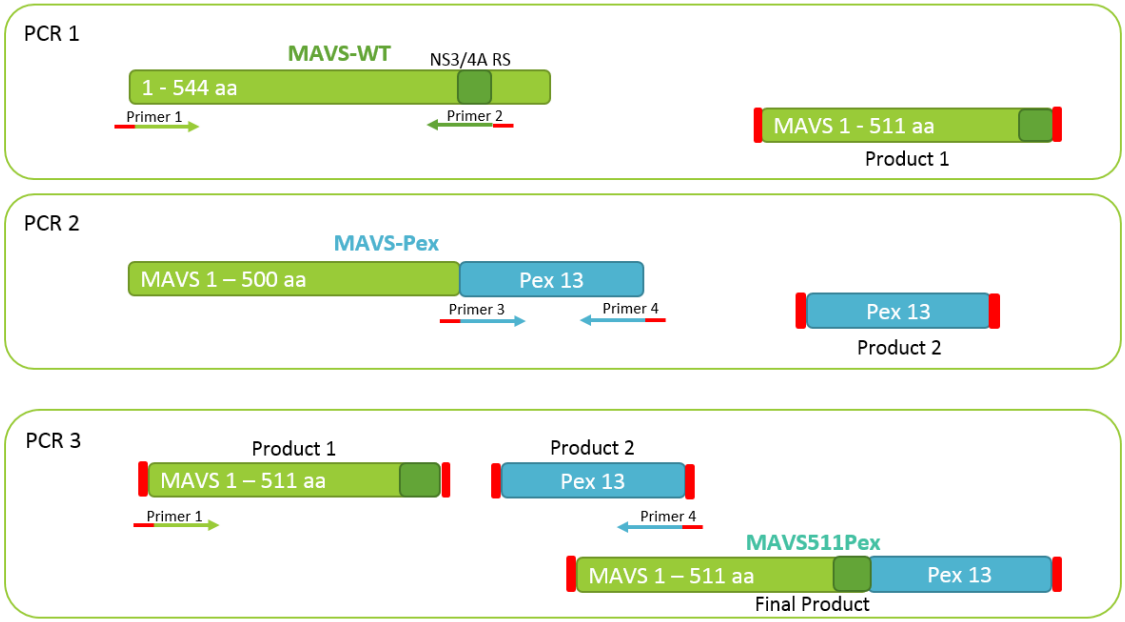

Figure 9 | Schematic representation of MAVS511Pex construction.

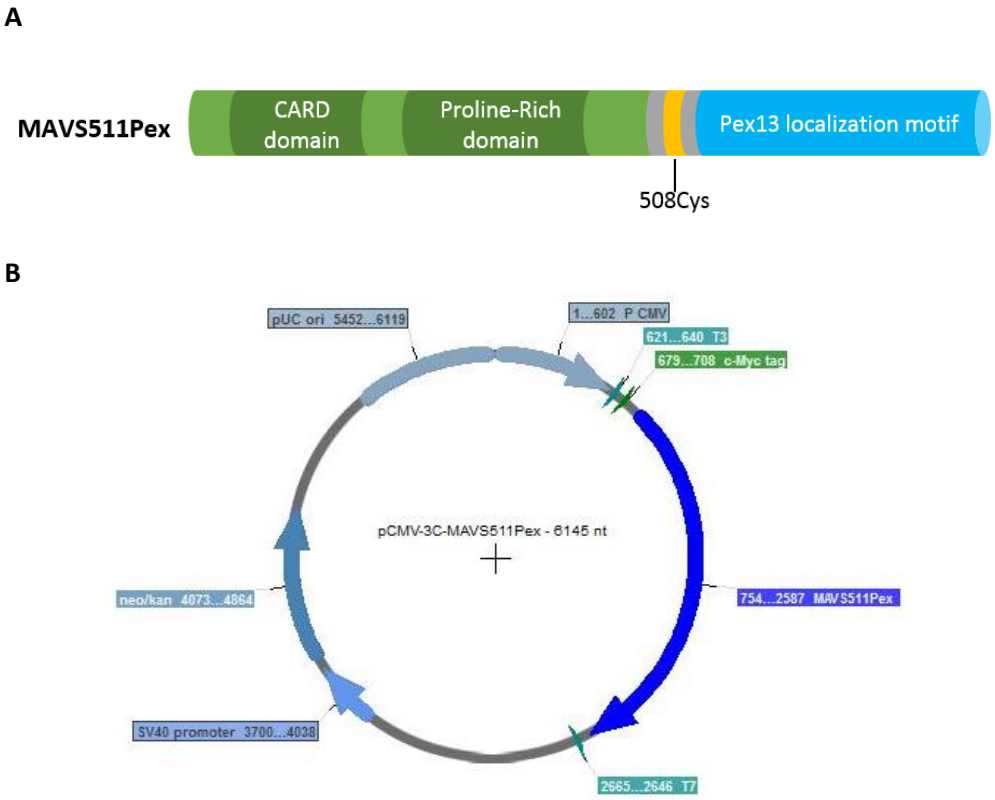

Figure 10 | MAVS511Pex. A) Schematic representation of MAVS511Pex domains. **B)** Schematic representation of plasmid pCMV-3C-MAVS511Pex.

To verify the localization of the newly made Myc-MAVS511Pex, the plasmid was overexpressed in mouse embryonic fibroblasts (MEFs) that were genetically altered to not express the MAVS protein in any organelle – MEF KO MAVS (Dixit et al 2010). These cells were then transfected by microporation with Myc-MAVS511Pex and were subjected to immunofluorescence analysis with antibodies against the peroxisomal marker PMP70 and Myc. Analysis by confocal microscopy showed that MAVS511Pex co-localized with peroxisomes (Figure 11).

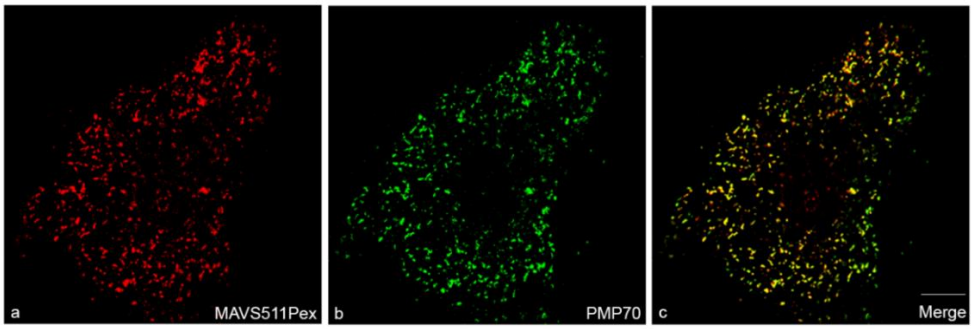

Figure 11 | MAVS511Pex co-localizes with peroxisomes. (a-c) Mefs KO MAVS cells transfected with Myc-MAVS511PEX; (a) Myc-MAVS511Pex, (b) PMP70, (c) merge image. Scale bar corresponds to 10µm.

HCV NS3/4A protease is a complex formed by two proteins: NS3 serine protease and the NS4A co-factor. Dr. Eliane Meurs (Institut Pasteur, France) kindly provided a NS3/4A construct inserted in the vector pcDNA3.1-/Hygro(-)T7-Tag-. However for this work we decided to insert it in a pEGFP-C1 vector in order to express the NS3/4A in conjugation with a GFP-tag (Figure 12A). We then amplified the NS3/4A sequence flanked with specific restriction sites in order to insert it into the pEGFP-C1. To confirm the expression and the cytosolic localization, GFP-NS3/4A was overexpressed in MEFs KO MAVS cells by Lipofectamine 3000. Cells were subjected to immunofluorescence analysis (Figure 12B) and photos were taken by confocal microscopy.

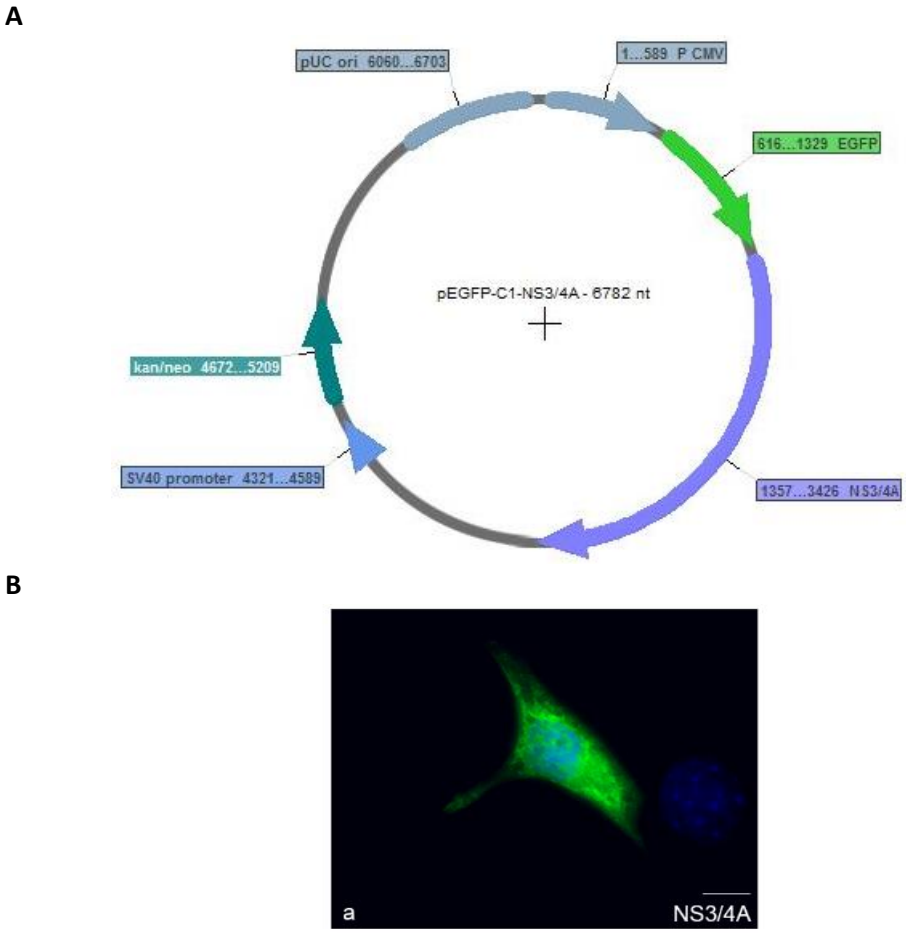

Figure 12 | GFP-NS3/4A. A) Graphic of pEGFP-C1-NS3/4A**. B)** GFP-NS3/4A expression**.** (a) Mefs KO MAVS cells transfected with GFP-NS3/4A. Scale bar corresponds to 10µm.

4.2. Peroxisomal MAVS is cleaved by HCV NS3/4A

The first reports showing the existence of MAVS at mitochondria also reported that this protein is targeted by the HCV NS3/4A complex (47,64,104). However, none of these reports investigated the effect of NS3/4A on the peroxisomal MAVS. To clarify whether the NS3/4A complex is able to similarly cleave the peroxisomal MAVS, Myc-MAVS511Pex was overexpressed in MEFs KO MAVS together with GFP-NS3/4A. Cells were co-transfected by microporation and fixed cells were subjected to immunolocalization with antibodies against Myc and Pex14, to mark Myc-MAVS511Pex and peroxisomes, respectively.

Analysing the co-expression of MAVS511Pex and NS3/4A by confocal microscopy it was clear that the MAVS localization changed from a peroxisomal to a cytosolic distribution, demonstrating that HCV NS3/4A is capable of cleaving the MAVS located at peroxisomes (Figure 13). In this image it is still possible to notice some co-localization between MAVS511Pex and peroxisomes (Figure 13: a,b,d – arrows indicate co-localization between Myc-MAVS511Pex and Pex14) as well as a co-localization between NS3/4A and peroxisomes (Figure X: b,c,d – full-head arrows indicate co-localization between GFP-NS3/4A and Pex14), indicating that at this point, not all the peroxisomal MAVS has yet been cleaved.

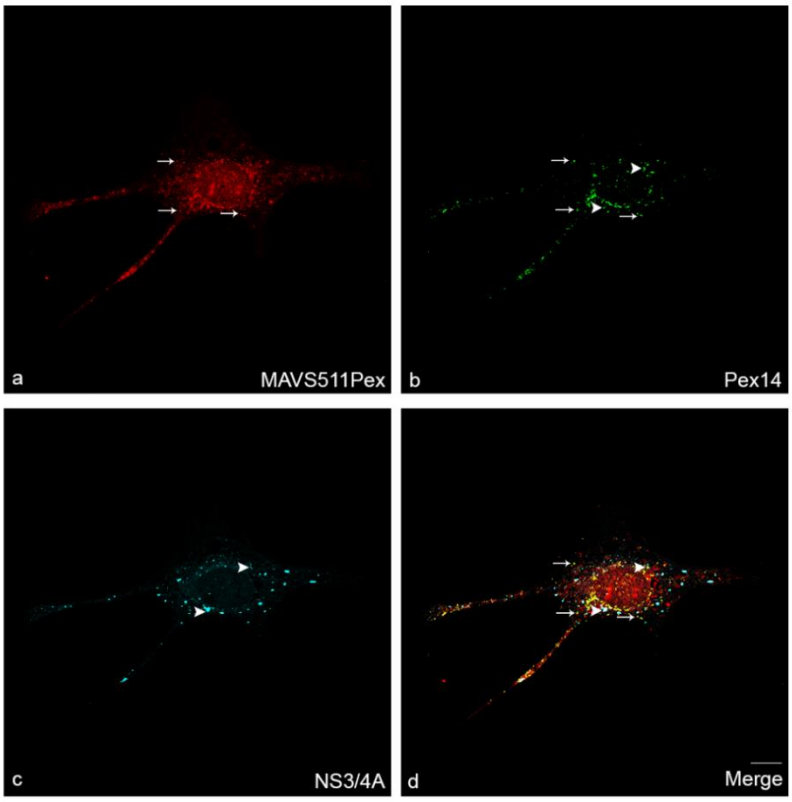

Figure 13 | Peroxisomal MAVS redistributes to cytosol after cleavage by HCV NS3/4A. (a-d) Mefs KO MAVS cells co-transfected with Myc-MAVS511Pex and GFP-NS3/4A; (a) Myc-MAVS511Pex, (b), Pex14, (c) GFP-NS3/4A, (d) and merge image. Arrows indicate co-localization between Myc-MAVS511Pex and Pex14. Full-head arrows indicate co-localization between Pex14 and GFP-NS3/4A. Scale bar corresponds to 10µm.

In parallel, the MAVS511Pex cleavage by NS3/4A was also analysed by immunoblotting. MEFs KO MAVS were co-transfected with Myc-MAVS511Pex and GFP-NS3/4A using Lipofectamine 3000. Alongside with MAVS511Pex, wild-type MAVS (Myc-MAVSWT) was also co-transfected with GFP-NS3/4A as a control for the cleavage. In both conditions, the HCV NS3/4A construct overexpression resulted in both wild-type MAVS and peroxisomal MAVS cleavage. The products of

the cleavage are faster-migrant fragments that were ≈5 to 12kDa shorter than Myc-MAVSWT and Myc-MAVS511Pex, respectively (Figure 14).

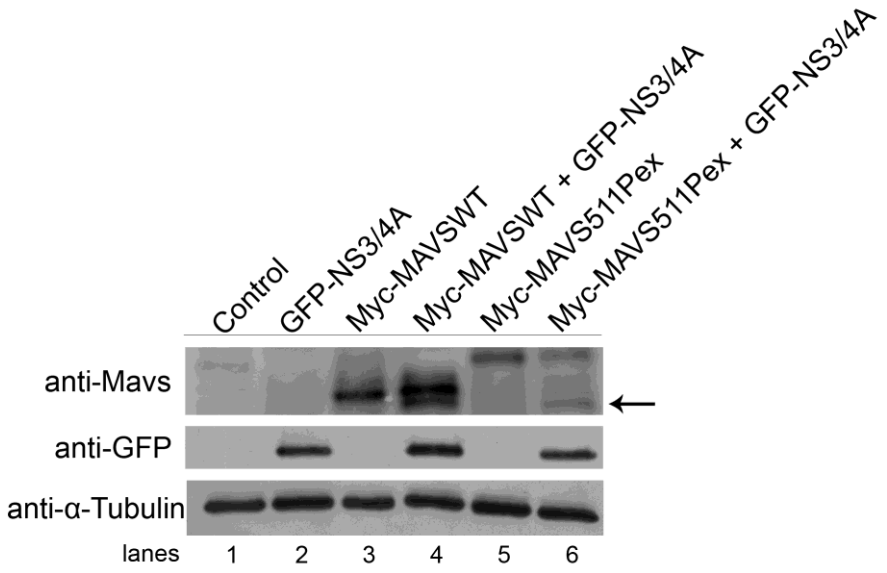

Figure 14 | Peroxisomal MAVS is cleaved by NS3/4A. Mefs KO MAVS cells co-transfected with Myc-MAVSWT or Myc-MAVS511Pex and GFP-NS3/4A. Arrow indicates the cleavage products of Myc-MAVSWT (lane 4) and Myc-MAVS511Pex (lane 6).

4.2. Peroxisomal MAVS cleavage by HCV NS3/4A impairs cellular antiviral response

In HCV infection, MAVS cleavage by NS3/4A complex leads to the inhibition of MAVS pathway and consequently to a decrease in type I IFN expression and ISGs production (64). Recent reports indicate that peroxisomal MAVS is responsible for the early induction of ISGs expression, such as viperin and IRF1. To examine the effect of NS3/4A on peroxisomal-MAVS, viperin and IRF1 expression were quantified by RT-qPCR. We once again co-transfected MAVS511Pex and NS3/4A in MEFs KO MAVS as, since these cells do not express MAVS neither in mitochondria or in peroxisomes, the ISG expression will solely depend on the peroxisomal-MAVS pathway. To stimulate the antiviral response we transfected a RIG-I-CARD construct that only encodes the CARD domains of RIG-I allowing their direct exposition to MAVS without needing a activator ligand for RIG-I, hence mimicking a viral infection (61). Thus, MEF KO MAVS cells were co-

transfected with Myc-MAVS511Pex and GFP-NS3/4A for 24 hours, and stimulated with GFP-RIG-I-CARD for 6 hours. For both IRF1 and viperin, a clear decrease in mRNA production was observed (Figure 15).

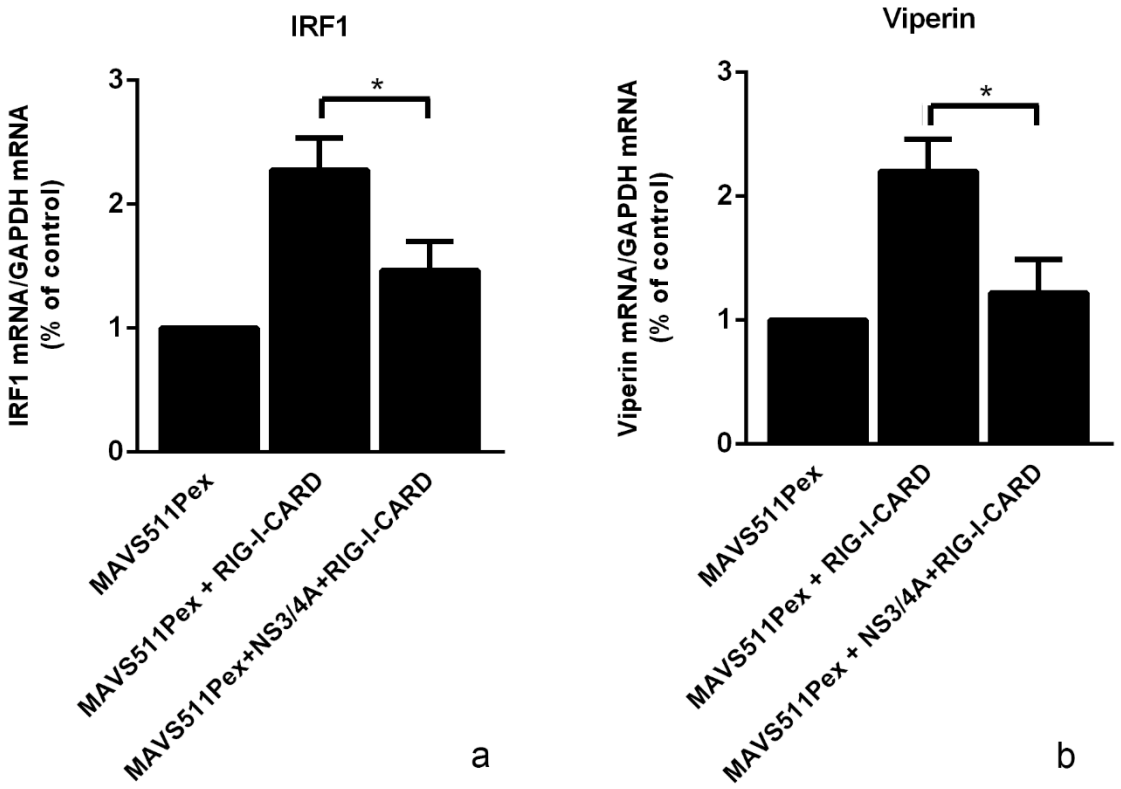

Figure 15 | Peroxisomal MAVS cleavage by NS3/4A impairs IRF1 and viperin expression. (a-b) Mefs KO MAVS cells were co-transfected with Myc-MAVS511Pex and GFP-NS3/4A and stimulated with GFP-RIG-I-CARD. mRNA expression of (a) IRF1 and (b) viperin was analysed by RT-qPCR. Data represents the means ±SEM of three independent experiments. Statistical analysis was performed using one-way ANOVA followed by Bonferroni's multiple comparison tests. Error bars represent SEM. *p≤0.05, compared with the MAVS511Pex condition considered as control.

V. Discussion

V. Discussion

During infection, cells detect non-self-molecules such as lipids, lipoproteins, proteins and nucleic acids, which present specific characteristics that allow their differentiation from the host cell molecules. Viruses release nucleic acids into the cytosol during viral replication, which are mainly recognized by cytosolic sensors from the RLR family that, when activated, transduce the signalling through the adaptor protein MAVS (57). The first reports on MAVS showed that it was located solely at the mitochondrial outer membrane but new data shows that it was also present at peroxisomes (63,67).

One of the studies that identified MAVS as an adaptor protein in RIG-I antiviral pathway also showed that HCV NS3/4A is able to cleave it in order to inhibit IRF3 activation (64). They identified the Cys-508 as the target residue for MAVS cleavage by NS3/4A. Other study that described the action of NS3/4A over MAVS reported the action of NS3/4A on the mitochondrial outer membrane (47).

In this study, we have developed a construct, the MAVS511Pex, that co-localized perfectly and solely with peroxisomes and allowed the specific study of the effect of HCV NS3/4A directly over the peroxisomal-MAVS pathway. Our results show that HCV NS3/4A is also capable of cleaving the MAVS localized at peroxisomes, as the presence of this viral protein resulted in the cleavage of MAVS at Cys-508 and dislocation of MAVS from peroxisomes to the cytosol, similarly to what had previously been shown to occur at the mitochondrial MAVS (63,64,68). Our data also shows some degree of co-localization of NS3/4A with peroxisomes, demonstrating its binding to the peroxisomal membrane in order to specifically cleave MAVS.

The reports on mitochondrial-MAVS inhibition by NS3/4A have shown that this causes an inhibition of the downstream signal transduction leading to a decrease in type I IFN expression and, consequent, inhibition of ISGs expression (47,64,105). However, these reports reflect the result of NS3/4A on the total MAVS present in the cell, until then thought to be only at mitochondria. In this work, besides showing that NS3/4A is also capable of cleaving MAVS exclusively at peroxisomes, we demonstrate that this cleavage clearly inhibits the peroxisomal-dependent downstream pathway by showing a decrease in IRF1 and viperin expression.

In our experiments, the MAVS pathway was stimulated by overexpression of a constitutively active form of RIG-I (RIG-I-CARD) where its CARD domain is exposed. Naturally, these results

should be validated upon HCV infection or in a specific cell model that stability expresses a HCV replicon.

The antiviral defence set by the activation of MAVS is dependent on its localization but both responses complement each other: the peroxisomal MAVS induces a rapid but short-termed IFN-independent response, whereas the mitochondrial MAVS activates a IFN-dependent response with delayed kinetics (67). The discovery of peroxisomal-MAVS targeting by HCV NS3/4A protease raised a question concerning the specificity of this targeting: could HCV set a specific inhibition at peroxisomal MAVS by cleaving it first, thus directly affecting the early antiviral response? As future work, one should investigate the sequence of events associated to the targeting of peroxisomal and mitochondrial MAVS by NS3/4A. For this, a similar construct to MAVS511Pex that targets this protein solely to mitochondria should be designed (MAVS511Mito). By co-transfecting the MAVS511Pex, MAVS511Mito and NS3/4A, one would be able to analyse which of the two proteins would be cleaved first. NS3/4A complex has several functions in HCV life cycle mainly due to its protease activity. Several other viruses produce similar complexes that impair MAVS pathways and some were already linked to its inhibition, such as Enterovirus (106), Poliovirus (106), Hepatitis A virus (107), and others. To better understand the importance of peroxisomal MAVS in the innate immune response against viruses it should be investigated whether these viruses also specifically target the peroxisomal MAVS impairing the associated antiviral signalling pathway.

VI. Final Remarks

VI. Final Remarks

6.1. Conclusions

Peroxisomes are important organelles in human health being responsible for many cellular metabolic pathways such as lipid metabolism. Their dysfunction or absence is associated with genetic disorders that can be fatal. The identification of MAVS at peroxisomes conferred to peroxisomes a new role in health and disease, particular in the innate immune response. MAVS is also present at mitochondria, accentuating the interconnection between these two organelles, long-time partners in several metabolic pathways.

HCV is a major human viral pathogen that infects hepatocytes and is highly dependent of on lipid metabolism. HCV has evolved specific mechanisms to overcome the cellular innate immune response. NS3/4A is a viral protease complex that targets adaptor proteins – MAVS and TRIF – coordinating the antiviral response induced by RLR and TLR3, respectively.

The main conclusion of this work is that the HCV NS3/4A protease cleaves peroxisomal MAVS, impairing the peroxisome-dependent cellular antiviral response (Figure 16) (47,64).

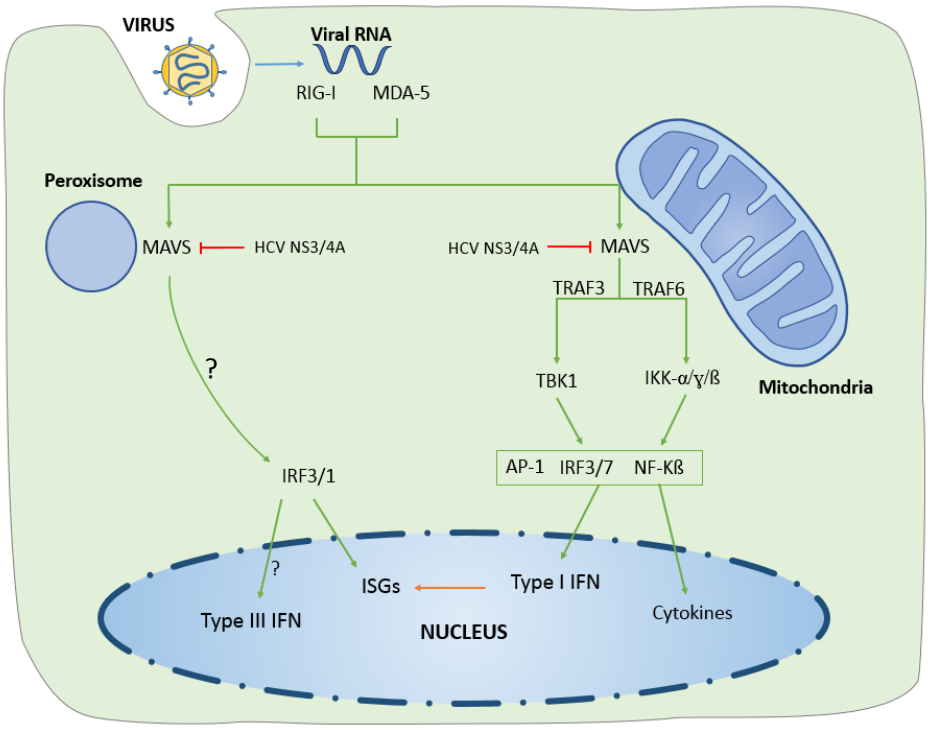

Figure 16 | Schematic representation of MAVS signalling pathway and interaction of HCV NS3/4A (67,71,72).

6.2. Publications resulting from this work

Ferreira A R, Magalhães A C, Gouveia A, Vieira M, Camões F, Kagan J, Ribeiro D. Hepatitis C virus NS3/4A inhibits peroxisomal MAVS-dependent antiviral signaling response. (manuscript in preparation to be submitted to Cell Host & Microbe)

VII. References

1. Choo QL, Kuo G, Weiner AJ, Overby LR, Bradley DW, Houghton M. Isolation of a cDNA clone derived from a blood-borne non-A, non-B viral hepatitis genome. Science. 1989 Apr 21;244(4902):359–62.

2. WHO | Hepatitis C [Internet]. Fact Sheet Nº 164. World Health Organization; 2014 [cited 2014 Jun 10]. Available from: http://www.who.int/mediacentre/factsheets/fs164/en/

3. Chen SL, Morgan TR. The natural history of hepatitis C virus (HCV) infection. Int J Med Sci. 2006 Jan;3(2):47–52.

4. Gottwein JM, Bukh J. Cutting the gordian knot-development and biological relevance of hepatitis C virus cell culture systems. Adv Virus Res. 2008 Jan;71(08):51–133.

5. Thomas E, Feld JJ, Li Q, Hu Z, Fried MW, Liang TJ. Ribavirin potentiates interferon action by augmenting interferon-stimulated gene induction in hepatitis C virus cell culture models. Hepatology. 2011 Jan;53(1):32–41.

6. Hofmann WP, Zeuzem S. A new standard of care for the treatment of chronic HCV infection. Nat Rev Gastroenterol Hepatol. Nature Publishing Group; 2011 May;8(5):257–64.

7. Schoggins JW, Rice CM. Innate Immune Responses to Hepatitis C Virus. In: Bartenschlager R, editor. Hepatitis C Virus: From Molecular Virology to Antiviral Therapy. Berlin, Heidelberg: Springer Berlin Heidelberg; 2013. p. 219–42.

8. Scheel TKH, Rice CM. Understanding the hepatitis C virus life cycle paves the way for highly effective therapies. Nat Med. Nature Publishing Group; 2013 Jul;19(7):837–49.

9. Levrero M. Viral hepatitis and liver cancer: the case of hepatitis C. Oncogene. 2006 Jun 26;25(27):3834–47.

10. Chevaliez S, Pawlotsky J-M. HCV Genome and Life Cycle. In: Tan S, editor. Hepatitis C Viruses: Genomes and Molecular Biology. Norfolk (UK): Horizon Bioscience; 2006. p. 5–47.

11. Suzuki T. Morphogenesis of infectious hepatitis C virus particles. Front Microbiol. 2012 Jan;3:38.

12. Catanese MT, Uryu K, Kopp M, Edwards TJ, Andrus L, Rice WJ, et al. Ultrastructural analysis of hepatitis C virus particles. Proc Natl Acad Sci U S A. 2013 Jun 4;110(23):9505–10.

13. Yanagi M, Purcell RH, Emerson SU, Bukh J. Transcripts from a single full-length cDNA clone of hepatitis C virus are infectious when directly transfected into the liver of a chimpanzee. Proc Natl Acad Sci U S A. 1997 Aug 5;94(16):8738–43.

14. Tariq H, Manzoor S, Parvaiz F, Javed F, Fatima K, Qadri I. An overview: in vitro models of HCV replication in different cell cultures. Infect Genet Evol. Elsevier B.V.; 2012 Jan;12(1):13–20.

15. Lohmann V. Hepatitis C: Methods and Protocols. Tang H, editor. Totowa, NJ: Humana Press; 2009;510:145–63.

16. Mukhopadhyay S, Kuhn RJ, Rossmann MG. A structural perspective of the flavivirus life cycle. Nat Rev Microbiol. 2005 Jan;3(1):13–22.

17. Merz A, Long G, Hiet M-S, Brügger B, Chlanda P, Andre P, et al. Biochemical and morphological properties of hepatitis C virus particles and determination of their lipidome. J Biol Chem. 2011 Jan 28;286(4):3018–32.

18. Gastaminza P, Dryden K a, Boyd B, Wood MR, Law M, Yeager M, et al. Ultrastructural and biophysical characterization of hepatitis C virus particles produced in cell culture. J Virol. 2010 Nov;84(21):10999–1009.

19. Bartenschlager R, Penin F, Lohmann V, André P. Assembly of infectious hepatitis C virus particles. Trends Microbiol. 2011 Feb;19(2):95–103.

20. Moradpour D, Penin F, Rice CM. Replication of hepatitis C virus. Nat Rev Microbiol. 2007 Jun;5(6):453–63.

21. Cocquerel L, Voisset C, Dubuisson J. Hepatitis C virus entry: potential receptors and their biological functions. J Gen Virol. 2006 May;87(Pt 5):1075–84.

22. Bartosch B, Cosset F-L. Cell entry of hepatitis C virus. Virology. 2006 Apr 25;348(1):1–12.

23. Zhu Y-Z, Qian X-J, Zhao P, Qi Z-T. How hepatitis C virus invades hepatocytes: the mystery of viral entry. World J Gastroenterol. 2014 Apr 7;20(13):3457–67.

24. Hoffman B, Liu Q. Hepatitis C viral protein translation: mechanisms and implications in developing antivirals. Liver Int. 2011 Nov;31(10):1449–67.

25. Shi ST, Lai MMC. HCV 5’ and 3' UTR: When Translation Meets Replication. In: Tan S, editor. Hepatitis C Viruses: Genomes and Molecular Biology. Norfolk (UK): Horizon Bioscience; 2006. p. 49–87.

26. Lindenbach BD, Rice CM. Unravelling hepatitis C virus replication from genome to function. Nature. 2005 Aug 18;436(7053):933–8.

27. Fauvelle C, Felmlee DJ, Baumert TF. Unraveling hepatitis C virus structure. Cell Res. Nature Publishing Group; 2014 Apr;24(4):385–6.

28. Kim CW, Chang K-M. Hepatitis C virus: virology and life cycle. Clin Mol Hepatol. 2013;(19):17–25.

29. Egger D, Wölk B, Gosert R, Blum HE, Moradpour D, Bienz K, et al. Expression of Hepatitis C Virus Proteins Induces Distinct Membrane Alterations Including a Candidate Viral Replication Complex. J Virol. 2002;76(12):5974–84.

30. Gosert R, Egger D, Lohmann V, Bartenschlager R, Blum HE, Bienz K, et al. Identification of the Hepatitis C Virus RNA Replication Complex in Huh-7 Cells Harboring Subgenomic Replicons. J Virol. 2003;77(9):5487–92.

31. Penin F, Dubuisson J, Rey F a, Moradpour D, Pawlotsky J-M. Structural biology of hepatitis C virus. Hepatology. 2004 Jan;39(1):5–19.

32. Bartenschlager R, Lohmann V. Replication of hepatitis C virus. J Gen Virol. 2000 Jul;81(Pt 7):1631–48.

33. Tang H, Grisé H. Cellular and molecular biology of HCV infection and hepatitis. Clin Sci (Lond). 2009 Jul;117(2):49–65.

34. Moriishi K, Matsuura Y. Host factors involved in the replication of hepatitis C virus. Rev Med Virol. 2007;17(5):343–54.

35. Enomoto N, Sato C. Hepatitis C virus quasispecies populations during chronic hepatitis C infection. Trends Microbiol. 1995 Nov;3(11):445–7.

36. Liu HM, Aizaki H, Machida K, Ou J-HJ, Lai MMC. Hepatitis C virus translation preferentially depends on active RNA replication. PLoS One. 2012 Jan;7(8):e43600.

37. Boulant S, Douglas MW, Moody L, Budkowska A, Targett-Adams P, McLauchlan J. Hepatitis C virus core protein induces lipid droplet redistribution in a microtubule- and dynein-dependent manner. Traffic. 2008 Aug;9(8):1268–82.

38. Suzuki T. Assembly of hepatitis C virus particles. Microbiol Immunol. 2011 Jan;55(1):12–8.

39. Tews BA, Popescu C-I, Dubuisson J. Last stop before exit - hepatitis C assembly and release as antiviral drug targets. Viruses. 2010 Aug;2(8):1782–803.

40. Targett-Adams P, Boulant S, Douglas MW, McLauchlan J. Lipid metabolism and HCV infection. Viruses. 2010 May;2(5):1195–217.

41. Lindebach BD, Rice CM. The ins and outs of hepatitis C virus entry and assembly. Nat Rev Microbiol. 2013;11(10):688–700.

42. Icard V, Diaz O, Scholtes C, Perrin-Cocon L, Ramière C, Bartenschlager R, et al. Secretion of hepatitis C virus envelope glycoproteins depends on assembly of apolipoprotein B positive lipoproteins. PLoS One. 2009 Jan;4(1):e4233.

43. Jones DM, McLauchlan J. Hepatitis C virus: assembly and release of virus particles. J Biol Chem. 2010 Jul 23;285(30):22733–9.

44. Lin C. HCV NS3-4A Serine Protease. In: Tan S-L, editor. Hepatitis C Viruses: Genomes and Molecular Biology. Norfolk (UK): Horizon Bioscience; 2006. p. 163–206.

45. Moradpour D, Penin F. Hepatitis C virus: From structure to Function. In: Bartenschlager R, editor. Hepatitis C Virus: From Molecular Virology to Antiviral Therapy. Springer-Verlag Berlin Heidelberg; 2013. p. 113–42.

46. Foy E, Li K, Wang C, Sumpter R, Ikeda M, Lemon SM, et al. Regulation of interferon regulatory factor-3 by the hepatitis C virus serine protease. Science. 2003 May 16;300(5622):1145–8.

47. Li X-D, Sun L, Seth RB, Pineda G, Chen ZJ. Hepatitis C virus protease NS3/4A cleaves mitochondrial antiviral signaling protein off the mitochondria to evade innate immunity. Proc Natl Acad Sci U S A. 2005 Dec 6;102(49):17717–22.

48. Foy E, Li K, Sumpter R, Loo Y-M, Johnson CL, Wang C, et al. Control of antiviral defenses through hepatitis C virus disruption of retinoic acid-inducible gene-I signaling. Proc Natl Acad Sci U S A. 2005 Feb 22;102(8):2986–91.

49. Mawatari S, Uto H, Ido A, Nakashima K, Suzuki T, Kanmura S, et al. Hepatitis C Virus NS3/4A Protease Inhibits Complement Activation by Cleaving Complement Component 4. PLoS One. 2013 Jan;8(12):e82094.

50. Gao B, Jeong W-I, Tian Z. Liver: An organ with predominant innate immunity. Hepatology. 2008 Mar;47(2):729–36.

51. Medzhitov R, Janeway C a. Innate Immunity: The Virtues of a Nonclonal System of Recognition. Cell. 1997 Oct;91(3):295–8.

52. Janeway C a, Medzhitov R. Innate immune recognition. Annu Rev Immunol. 2002 Jan;20(2):197–216.

53. Seth RB, Sun L, Chen ZJ. Antiviral innate immunity pathways. Cell Res. 2006 Feb;16(2):141–7.

54. Thompson MR, Kaminski JJ, Kurt-Jones E a, Fitzgerald K a. Pattern recognition receptors and the innate immune response to viral infection. Viruses. 2011 Jun;3(6):920–40.

55. Kawai T, Akira S. Innate immune recognition of viral infection. Nat Immunol. 2006 Feb;7(2):131–7.

56. Ranjan P, Bowzard JB, Schwerzmann JW, Jeisy-Scott V, Fujita T, Sambhara S. Cytoplasmic nucleic acid sensors in antiviral immunity. Trends Mol Med. 2009 Aug;15(8):359–68.

57. Yoneyama M, Kikuchi M, Matsumoto K, Imaizumi T, Miyagishi M, Taira K, et al. Shared and Unique Functions of the DExD/H-Box Helicases RIG-I, MDA5, and LGP2 in Antiviral Innate Immunity. J Immunol. 2005 Aug 22;175(5):2851–8.

58. Kaisho T, Akira S. Toll-like receptor function and signaling. J Allergy Clin Immunol. 2006 May;117(5):979–87.

59. Wilkins C, Gale M. Recognition of viruses by cytoplasmic sensors. Curr Opin Immunol. Elsevier Ltd; 2010 Feb;22(1):41–7.

60. Paludan SR, Bowie AG. Immune sensing of DNA. Immunity. Elsevier Inc.; 2013 May 23;38(5):870–80.

61. Yoneyama M, Kikuchi M, Natsukawa T, Shinobu N, Imaizumi T, Miyagishi M, et al. The RNA helicase RIG-I has an essential function in double-stranded RNA-induced innate antiviral responses. Nat Immunol. 2004 Jul;5(7):730–7.

62. Saito T, Gale M. Differential recognition of double-stranded RNA by RIG-I-like receptors in antiviral immunity. J Exp Med. 2008 Jul 7;205(7):1523–7.

63. Seth RB, Sun L, Ea C-K, Chen ZJ. Identification and characterization of MAVS, a mitochondrial antiviral signaling protein that activates NF-kappaB and IRF 3. Cell. 2005 Sep 9;122(5):669–82.

64. Meylan E, Curran J, Hofmann K, Moradpour D, Binder M, Bartenschlager R, et al. Cardif is an adaptor protein in the RIG-I antiviral pathway and is targeted by hepatitis C virus. Nature. 2005 Oct;437(7062):1167–72.

65. Kawai T, Takahashi K, Sato S, Coban C, Kumar H, Kato H, et al. IPS-1, an adaptor triggering RIG-I- and Mda5-mediated type I interferon induction. Nat Immunol. 2005 Oct;6(10):981–8.

66. Xu L-G, Wang Y-Y, Han K-J, Li L-Y, Zhai Z, Shu H-B. VISA is an adapter protein required for virus-triggered IFN-beta signaling. Mol Cell. 2005 Sep 16;19(6):727–40.

67. Dixit E, Boulant S, Zhang Y, Lee ASY, Odendall C, Shum B, et al. Peroxisomes are signaling platforms for antiviral innate immunity. Cell. Elsevier Ltd; 2010 May 14;141(4):668–81.

68. Horner SM, Liu HM, Park HS, Briley J, Gale M. Mitochondrial-associated endoplasmic reticulum membranes (MAM) form innate immune synapses and are targeted by hepatitis C virus. Proc Natl Acad Sci U S A. 2011 Aug;108(35):14590–5.

69. Hou F, Sun L, Zheng H, Skaug B, Jiang Q-X, Chen ZJ. MAVS forms functional prion-like aggregates to activate and propagate antiviral innate immune response. Cell. Elsevier Inc.; 2011 Aug 5;146(3):448–61.

70. Xu H, He X, Zheng H, Huang LJ, Hou F, Yu Z, et al. Structural basis for the prion-like MAVS filaments in antiviral innate immunity. 2014;5:1–25.

71. Odendall C, Dixit E, Stavru F, Bierne H, Franz KM, Durbin AF, et al. Diverse intracellular pathogens activate type III interferon expression from peroxisomes. Nat Immunol. Nature Publishing Group; 2014 Jun 22;15(8):717–26.

72. Onoguchi K, Yoneyama M, Takemura A, Akira S, Taniguchi T, Namiki H, et al. Viral infections activate types I and III interferon genes through a common mechanism. J Biol Chem. 2007 Mar 9;282(10):7576–81.

73. Hiscott J. Convergence of the NF-kappaB and IRF pathways in the regulation of the innate antiviral response. Cytokine Growth Factor Rev. 2007 Jan;18(5-6):483–90.

74. Loo Y-M, Owen DM, Li K, Erickson AK, Johnson CL, Fish PM, et al. Viral and therapeutic control of IFN-beta promoter stimulator 1 during hepatitis C virus infection. Proc Natl Acad Sci U S A. 2006 Apr 11;103(15):6001–6.

75. Metz P, Reuter A, Bender S, Bartenschlager R. Interferon-stimulated genes and their role in controlling hepatitis C virus. J Hepatol. European Association for the Study of the Liver; 2013 Aug 8;59(6):1331–41.

76. Horner SM, Gale M. Regulation of hepatic innate immunity by hepatitis C virus. Nat Med. Nature Publishing Group; 2013 Jul;19(7):879–88.

77. Heim MH. Innate immunity and HCV. J Hepatol. European Association for the Study of the Liver; 2013 Mar;58(3):564–74.

78. Park S-H, Rehermann B. Immune responses to HCV and other hepatitis viruses. Immunity. Elsevier Inc.; 2014 Jan 16;40(1):13–24.

79. Lazarow PB, Fujiki Y. Biogenesis of peroxisomes. Annu Rev Cell Biol. 1985 Jan;1:489–530.

80. Schrader M, Grille S, Fahimi HD, Islinger M. Peroxisome Interactions and Cross-Talk with Other Subcellular Compartments in Animal Cells. In: del Rio LA, editor. Peroxisomes and their Key Role in Cellular Signaling and Metabolism. Dordrecht: Springer Science & Business Media; 2013. p. 1–23.

81. Lodhi IJ, Semenkovich CF. Peroxisomes: A Nexus for Lipid Metabolism and Cellular Signaling. Cell Metab. Elsevier Inc.; 2014 Feb 5;19(3):380–92.

82. Islinger M, Schrader M. Peroxisomes. Curr Biol. 2011 Oct 11;21(19):R800–1.

83. Ribeiro D, Castro I, Fahimi HD, Schrader M. Peroxisome morphology in pathology. Histhology and Histhopathology. 2012;27(6):661–76.

84. Aubourg P, Wanders R. Peroxisomal disorders. 1st ed. Handbook of clinical neurology. Elsevier B.V.; 2013.

85. Wanders RJA. Metabolic functions of peroxisomes in health and disease. Biochimie. Elsevier Masson SAS; 2014 Mar;98:36–44.

86. Islinger M, Grille S, Fahimi HD, Schrader M. The peroxisome: an update on mysteries. Histochem Cell Biol. 2012 May;137(5):547–74.

87. Rucktäschel R, Halbach A, Girzalsky W, Rottensteiner H, Erdmann R. De novo synthesis of peroxisomes upon mitochondrial targeting of Pex3p. Eur J Cell Biol. 2010 Dec;89(12):947–54.

88. Schrader M, Bonekamp N a, Islinger M. Fission and proliferation of peroxisomes. Biochim Biophys Acta. Elsevier B.V.; 2012 Sep;1822(9):1343–57.

89. Van der Zand A, Tabak HF. Peroxisomes: offshoots of the ER. Curr Opin Cell Biol. Elsevier Ltd; 2013 Aug;25(4):449–54.

90. Platta HW, Hagen S, Reidick C, Erdmann R. The peroxisomal receptor dislocation pathway: To the exportomer and beyond. Biochimie. Elsevier Masson SAS; 2014 Mar;98C:16–28.

91. Schrader M, Fahimi HD. The peroxisome: still a mysterious organelle. Histochem Cell Biol. 2008 Apr;129(4):421–40.

92. Yorimitsu T, Klionsky DJ. Autophagy: molecular machinery for self-eating. Cell Death Differ. 2005 Nov;12:1542–52.

93. De Duve C, Baudhuin P. Peroxisomes (microbodies and related particles). Physiol Rev. 1966 Apr 1;46(2):323–57.

94. Poirier Y, Antonenkov VD, Glumoff T, Hiltunen JK. Peroxisomal beta-oxidation - a metabolic pathway with multiple functions. Biochim Biophys Acta. 2006 Dec;1763(12):1413–26.

95. Wanders RJA. Peroxisomes in human health and disease: metabolic pathways, metabolite transport, interplay with other organelles and signal transduction. In: del Río LA, editor. Peroxisomes and their Key Role in Cellular Signaling and Metabolism. Vol 69. 2: Springer Science & Business Media; 2013. p. 23–44.

96. Delille HK, Bonekamp NA, Schrader M. Peroxisomes and disease - an overview. Int J Biomed Sci. 2006 Dec;2(4):308–14.

97. Bonekamp NA, Völkl A, Fahimi HD, Schrader M. Reactive oxygen species and peroxisomes: struggling for balance. Biofactors. 35(4):346–55.

98. Camões F, Islinger M, Guimarães SC, Kilaru S, Schuster M, Godinho LF, et al. New insights into the peroxisomal protein inventory: Acyl-CoA oxidases and -dehydrogenases are an ancient feature of peroxisomes. Biochim Biophys Acta. 2014 Oct 13;1853(1):111–25.

99. Del Río LA, Sandalio LM, Corpas FJ, Palma JM, Barroso JB. Reactive oxygen species and reactive nitrogen species in peroxisomes. Production, scavenging, and role in cell signaling. Plant Physiol. 2006 Jun;141(2):330–5.

100. Kirkman HN, Gaetani GF. Mammalian catalase: a venerable enzyme with new mysteries. Trends Biochem Sci. 2007 Jan;32(1):44–50.

101. Camões F, Bonekamp NA, Delille HK, Schrader M. Organelle dynamics and dysfunction: A closer link between peroxisomes and mitochondria. J Inherit Metab Dis. 2009 Apr;32(2):163–80.

102. Lazarow PB. Viruses exploiting peroxisomes. Curr Opin Microbiol. Elsevier Ltd; 2011 Aug;14(4):458–69.

103. Odendall C, Kagan JC. Peroxisomes and the Antiviral Responses of Mammalian Cells. In: del Río LA, editor. Peroxisomes and their Role in Cellular Signalling. Dordrecht: Springer Netherlands; 2013. p. 67–75.

104. Horner SM, Liu HM, Park HS, Briley J, Gale M. Mitochondial-associated endoplasmic reticulum membranes (MAM) form innate immune synapses and are targeted by hepatitis C virus. Proc Natl Acad Sci. 2011;108(35):14590–5.

105. Bellecave P, Sarasin-Filipowicz M, Donzé O, Kennel A, Gouttenoire J, Meylan E, et al. Cleavage of mitochondrial antiviral signaling protein in the liver of patients with chronic hepatitis C correlates with a reduced activation of the endogenous interferon system. Hepatology. 2010 Apr;51(4):1127–36.

106. Feng Q, Langereis M a, Lork M, Nguyen M, Hato S V, Lanke K, et al. Enterovirus 2Apro targets MDA5 and MAVS in infected cells. J Virol. 2014 Mar;88(6):3369–78.

107. Yang Y, Liang Y, Qu L, Chen Z, Yi M, Li K, et al. Disruption of innate immunity due to mitochondrial targeting of a picornaviral protease precursor. Proc Natl Acad Sci U S A. 2007 Apr 24;104(17):7253–8.